Evaluation of the Removal of Perfluoroalkyl Substances from Aqueous Matrices in the Presence of Zerovalent Iron

by

Janis Rachel Baldwin

A thesis

presented to the University of Waterloo

in fulfilment of the

thesis requirement for the degree of

Master of Science

in

Earth Sciences (Water)

Waterloo, Ontario, Canada, 2018

Author's Declaration

I hereby declare that I am the sole author of this thesis. This is a true copy of the thesis, including any required final revisions, as accepted by my examiners.

I understand that my thesis may be made electronically available to the public.

Abstract

Per- and polyfluoroalkyl substances (PFASs) are a class of persistent organic pollutants present in the environment that pose a threat to human health. PFASs primarily reside within aqueous phases and are present in groundwater environments. Perfluorooctane sulfonic acid (PFOS) and perfluorooctanoic acid (PFOA) are the most predominant PFASs. Remediation techniques focus on oxidation and sorption methods, both of which lack efficacy for all PFASs. There are few studies on reduction treatments such as zerovalent iron (ZVI), which demonstrate potential for both PFOS and PFOA removal and can be applied in subsurface environments.

This thesis describes laboratory batch experiments that evaluate PFOS and PFOA removal in the presence of ZVI under a range of physical and geochemical conditions. Mechanisms of removal are explored utilizing PFAS mass balances based on a series of analyses that include aqueous phase fluoride and PFAS short chains, and PFAS extractions from the iron surface. Solid iron phase characterization provides supporting information regarding PFAS interaction with the iron surface.

Laboratory batch experiments with PFOS in the presence of granular ZVI were conducted under combinations of initial pH (pH 2.0 and 6.6), temperature ($\sim$22°C and 60°C) and ZVI dosage (179 and 1792 mM). PFOS removal was enhanced under low initial pH likely due to a greater abundance of iron oxides compared to higher pH conditions. Higher temperatures also enhanced PFOS removal. PFOS removal by sorption generally increased under low pH and high ZVI dosed conditions, suggesting the abundance of iron oxides and surface area may play an important role.

Laboratory batch experiments of PFOS and PFOA in the presence of zerovalent iron nanoparticles (nZVI) were conducted under combinations of initial pH (pH 2.0 and 8.3) and coating (uncoated and palladium-coated). The iron phase likely changed over time, as there was some release of PFOS and PFOA into aqueous solution com-

pared to earlier sampling times. The presence of a palladium coating appeared to minimize the effects of iron corrosion, as PFOS and PFOA were released to a lesser degree at later time points compared to uncoated nZVI. PFOS and PFOA removal is likely dominated by electrostatic interaction, however functional group interaction with the iron surface may also play an important role.

Acknowledgements

I would like to thank my supervisor Carol Ptacek for igniting my curiosity of emerging contaminants in groundwater and I appreciate the freedom I had to explore research options. Her support and kindness were invaluable at times when I needed it the most. I would also like to extend my gratitude to my committee members David Blowes and Neil Thomson for their provision of valuable input throughout my research ventures.

I would like to thank YingYing Liu, Laura Groza, Jing Ma, Krista Elena and Tim LeShuk for their help with my early experiments and analyses as it was a difficult transition from an undergraduate to a graduate research student. I am grateful to Janice Cooper for her teamwork as we worked through some difficult problems, as well as for my GGR colleagues, friends and family for their support along the way.

I am very appreciative to my funding sources, namely Natural Sciences and Engineering Research Council (NSERC) of Canada Discovery Grant, NSERC of Canada Collaborative Research and Development Grant, American Petroleum Institute, Ontario Graduate Scholarship and the Royal Bank of Canada Blue Water Project for making this research possible.

Table of Contents

List of Figures

List of Tables

List of Abbreviations

AFFF = aqueous film-forming foams

AOP = advanced oxidation processes

EMV = electron multiplier voltage

FTOH = fluorotelomer alcohol

HLB = hydrophilic hydrophobic balance

HPLC-MS/MS = high-performance liquid chromatography tandem mass spectrometry

MDL = method detection limit

nZVI = zerovalent iron nanoparticles

PdnZVI = palladium-coated zerovalent iron nanoparticles

PFAS = per- and polyfluoroalkyl substance

PFBS = perfluorobutane sulfonic acid

PFCA = perfluoroalkyl carboxylic acid

PFHpS = perfluoroheptane sulfonic acid

PFHxS = perfluorohexane sulfonic acid

PFOA = perfluorooctanoic acid

PFOS = perfluorooctane sulfonic acid

PFSA = perfluoroalkyl sulfonic acid

PTFE = polytetrafluoroethylene

SPE = solid phase extraction

TEM = transmission electron microscopy

UV = ultraviolet

WWTP = waste water treatment plant

ZVI = zerovalent iron

Chapter 1

Introduction

1.1 Background

Per- and polyfluoroalkyl substances (PFASs) are a diverse group of persistent organic pollutants that are used in a wide variety of industrial applications and are detected ubiquitously in the environment (Buck et al., 2011). PFASs are hydrocarbon chains which have all or at least one hydrogen substituted with fluorine and exhibit hydrophobic properties while the addition of a hydrophilic group at the end of the chain adds hydrophilic properties (Buck et al., 2011). The dual hydrophilic-hydrophobic nature and high thermal and chemical stability of PFASs make them extremely versatile for a wide variety of applications across the aerospace, automotive, semiconductor, apparel/textiles, chemical manufacturing and building/construction industries (US EPA, 2009). They are used in many everyday products due to their stain, water, and soil-repellant properties as coatings for carpets, clothing, paper, non-stick cookware, food packaging and paints (Skutlarek et al., 2006). Another common application is their use in aqueous film-forming foams (AFFFs) to extinguish liquid-fuel fires, after which PFASs often leach into groundwater (Moody et al., 2003).

PFASs encompass a wide range of compounds, however, the primary groups are perfluoroalkyl carboxylic acids ($C_nF_{2n+1}COOH$, PFCAs) and perfluoroalkyl sulfonic acids ($C_nF_{2n+1}SO_3H$, PFSAs) (Buck et al., 2011). An overview of PFCAs and PFSAs is presented in Table 1.1. Regulatory agencies are primarily concerned with long-chain ($n \geq 6$ for PFSAs, $n \geq 7$ for PFCAs) PFASs, as they are more bioaccumulative than their short-chain counterparts. The most discussed PFASs in the literature and regulations are perfluorooctanoic acid (PFOA) and perfluorooctane sulfonic acid (PFOS), as they are widely prevalent in aqueous environments (Buck et al., 2011). The properties of PFOS and PFOA are presented in Table 1.2. PFOS can cause neuroendocrine effects, as it is mobile across blood-brain and placental barriers (Austin et al., 2003). High-dose studies indicate exposure of rodents to PFASs increases the risk of cancer,

developmental delays, endocrine disruption, immunotoxicity and neonatal mortality (Jensen & Leffers, 2008; Lau et al., 2007, 2006). In wildlife species, PFOS is found to exceed guidelines in fish and bird eggs with a bioaccumulation factor of 1000 to 4000 (Gewurtz et al., 2013).

Current drinking water regulations for PFASs mainly target PFOS and PFOA (Table 1.3). In addition to the recommended drinking water concentrations, the US has a 2010/2015 PFOA Stewardship Program which involves a commitment to a 95% reduction by 2010 from the year 2000 baseline, and elimination by 2015 (US EPA, 2009). In 2008 Canadian regulations were established to prohibit the manufacture, use, sale and import of PFOS, its salts and precursors. In 2013, AFFFs containing PFASs were only permitted for use until July 2013 (Environment Canada, 2013). In 2009, PFOS was added to the Stockholm Convention List of Persistent Organic Pollutants, which restricts manufacturing and use (Gewurtz et al., 2013; Jin & Zhang, 2015).

The main routes of PFAS entry in the environment are through industrial and manufacturing plants of PFASs, degradation of fluorotelomer alcohol (FTOH) precursors, wastewater treatment plant (WWTP) effluent, use of AFFFs, and landfill leachate (US EPA, 2009). In the Ohio River near the Washington Works Plant (Dupont) in West Virginia, US, PFOA concentrations up to 13.3 μg L^{-1} were measured, resulting in 60 to 75 times higher blood levels of PFOA in local residents compared to the general population (Hoffman et al., 2010). Based on sampling of Ontario, Canada sewage treatment plants, PFOA concentrations range from 7 to 55 ng L^{-1} in the effluent with no indication of removal based on constant influent and effluent concentrations (Yu et al., 2009; Stock et al., 2009). Groundwater collected from the Tyndall (FL, USA) and Wurtsmith (MI, USA) Air Force Bases contained 125 to 7,090 μg L^{-1} of PFCAs (C_6 to C_8) after 7 to 10 years of inactivity from

fire-training using AFFFs (Moody & Field, 1999).

Most PFASs have a low vapour pressure and thus reside in aqueous phases or sorb to solid phases (Prevedouros et al., 2006). PFOS and PFOA are primarily found in their anionic form under most environmental conditions due to low pKa values (Yu et al., 2009). PFAS sorption in the natural environment is proportional to the fraction of organic carbon; where solid-phase organic carbon contents are relatively low, PFOS and PFOA are transported mainly in the dissolved phase and easily desorb from sediments (Ahrens et al., 2011). Many PFASs are extremely resistant to microbial degradation under natural conditions (Sáez et al., 2008). In a 285-day outdoor microcosm study under natural conditions, no reduction in PFOS concentration was observed (Boudreau et al., 2003).

1.2 Treatment Methods

Sorption is one of the most investigated mechanisms for PFAS removal due to its applicability for use at WWTPs and lack of harmful by-products. Within 10 minutes between 20 and 40% of PFASs adsorb onto granular activated carbon and between 60 and 90% on powdered activated carbon (Hansen et al., 2010). A variety of alternative materials to activated carbon have been evaluated, including black carbon, biochar, zeolite and activated sludge, but are not as effective as activated carbon for PFAS removal (Chen et al., 2009; Kupryianchyk et al., 2015; Liu et al., 2016; Ochoa-Herrera & Sierra-Alvarez, 2008). The presence of Ca^{2+} ions and low pH conditions may enhance PFAS sorption as Ca^{2+} and H^{+} ions can reduce repulsion between organic matter and the anionic functional group of PFASs (Arvaniti et al., 2014; Chen et al., 2009).

Advanced oxidation processes (AOPs) including O_3, O_3/UV, O_3/H_2O_2, H_2O_2/Fe(II)

are applied to degrade persistent organic pollutants but were ineffective in the destruction of PFOS (Schröder & Meesters, 2005). AOPs primarily generate hydroxyl radicals which act through hydrogen abstraction. PFASs do not have any hydrogen atoms to abstract, rendering the hydroxyl radicals ineffective. Persulfate ($S_2O_8^{2-}$) in combination with various activation methods is a well-researched oxidant for PFAS degradation. Persulfate can be activated with heat, ultraviolet (UV) light or transition metals (M^{n+}) to generate sulfate radicals through the following mechanisms (Tsitonaki et al., 2010; Yin et al., 2016):

$$S_2O_8^{2-} + heat/UV \rightarrow 2SO_4^{\bullet -} \tag{1.1}$$

$$S_2O_8^{2-} + M^{n+} \rightarrow SO_4^{\bullet -} + SO_4^{2-} + M^{n+1} \tag{1.2}$$

Under acidic pH conditions, protons act as a catalyst for the formation of sulfate radicals ($SO_4^{\bullet -}$):

$$S_2O_8^{2-} + H^+ \rightarrow HS_2O_8^- \tag{1.3}$$

$$HS_2O_8^- \rightarrow SO_4^{\bullet -} + SO_4^{2-} + H^+ \tag{1.4}$$

Persulfate can be activated under alkaline pH, however, the conversion of sulfate radicals to hydroxyl radicals increases, reducing efficacy for PFASs removal. PFOA was removed in the presence of persulfate activated by heat, UV, and zerovalent iron (ZVI) while PFOS removal was minimal (Lee et al., 2010, 2012, 2009; Liu et al., 2012a; Park et al., 2016; Yang et al., 2013; Yin et al., 2016). Removal of PFOA is enhanced by persulfate under low pH conditions, regardless of activator, likely due to the increased presence of sulfate radicals (Eqn. 1.3, 1.4) (Yin et al., 2016). PFOS

removal is minimal and does not appear to change regardless of pH condition in the presence of persulfate, suggesting sulfate radicals may not be effective for PFOS destruction (Park et al., 2016).

Reductive dehalogenation is utilized as a treatment technology for many persistent halogenated organic contaminants (Vecitis et al., 2009). Advanced reductive processes involve highly reactive, nonselective reducing nucleophiles or radicals such as hydrated electrons, $H^{\bullet}$ and $SO_3^{\bullet -}$ (Merino et al., 2016). Jin & Zhang (2015), examined the application of hydrated electrons in an anoxic alkaline solution under vacuum UV light, which led to PFOS defluorination.Very little PFOA removal with sulfite and dithionite under UV light occurs and requires highly alkaline conditions in a UV-potassium iodide system for removal (Qu et al., 2014; Vellanki et al., 2013).

ZVI is also an effective electron donor (Li et al., 2006):

$$Fe(0) \longrightarrow Fe^{2+} + 2e^{-} \tag{1.5}$$

Highly electronegative halogens such as F^{-} may accept the electrons and PFASs could potentially undergo reductive defluorination. Hori et al. (2006) achieved up to 51% PFOS defluorination using ZVI in subcritical water (350°C) and high pressure (23 MPa) conditions after 6 hours of exposure. Zerovalent iron nanoparticles (nZVI) also remove PFOS and PFOA to a significant degree, with magnesium amino-clay and palladium coatings (Arvaniti et al., 2015; Park et al., 2017). While PFAS removal methods such as sorption and oxidation are extensively studied, the application of reduction methods requires more investigation as they demonstrate potential as effective treatment materials.

1.3 Research Objectives

PFASs are a diverse group of compounds, whose removal is largely dependent on the properties of the target compound and the treatment material removal mechanism. More investigation into alternative mechanisms for PFAS removal is needed. Documentation of reductive treatments is comparatively lacking in the literature and shows signs of promise based on the studies published to date. The primary goal of this research was to examine the treatment effectiveness of ZVI-based treatments for PFOS and PFOA removal in aqueous matrices.

Batch experiments were used to evaluate potential removal of PFOS/PFOA under varying controlled conditions. High-performance liquid chromatography tandem mass spectrometry (HPLC-MS/MS) analysis of PFOS/PFOA was used to quantify the effectiveness of the treatment for PFOS/PFOA degradation. Supporting analyses of F^- and PFAS short-chains determined the extent of mineralization while the degree of sorption was determined by analyzing PFOS released from the surface of ZVI grains.

The hypothesis for the proposed research is that the degradation of PFOS and PFOA will require specific conditions in the presence of ZVI to generate sufficient reactive electrons. Based on previous literature of ZVI and PFASs, optimal conditions consistently require low pH and high dosage while temperature influence is unclear. Certain types of coatings are likely to enhance the reactivity of ZVI. Assuming the strength of the reagent is sufficient to overcome the bond dissociation energy of the C-F bond, complete mineralization will occur if sufficient time and quantity of active reagent and conditions are sustained.

The research will contribute towards understanding the mechanisms involved in PFOS and PFOA removal and the potential applicability of treatments in the subsurface.

1.4 Thesis Organization

This thesis is structured as two research studies related to the objectives outlined. The first study, presented as Chapter 2, describes laboratory batch experiments conducted to evaluate the removal of PFOS in the presence of granular ZVI under a combination of conditions, with initial pH, temperature, and ZVI dosage as variables. The second study, presented as Chapter 3, describes laboratory batch experiments conducted to evaluate the removal of PFOS and PFOA in the presence of nZVI under a combination of conditions, with initial pH and nZVI coating as variables. The final chapter, Chapter 4, presents a summary of findings from both studies and implications.

Table 1.1 Overview of PFCA and PFSA chemical names, acronyms and molecular formulas.

Chemical Name	**Acronym**	**Molecular Formula**
Perfluoroalkyl Carboxylic Acids (PFCAs)		
Perfluoropentanoic acid	PFPeA	C_4F_9COOH
Perfluorohexanoic acid	PFHxA	$C_5F_{11}COOH$
Perfluoroheptanoic acid	PFHpA	$C_6F_{13}COOH$
Perfluorooctanoic acid	PFOA	$C_7F_{15}COOH$
Perfluorononanoic acid	PFNA	$C_8F_{17}COOH$
Perfluorodecanoic acid	PFDA	$C_9F_{19}COOH$
Perfluoroundecanoic acid	PFUnA	$C_{10}F_{21}COOH$
Perfluorododecanoic acid	PFDoA	$C_{11}F_{23}COOH$
Perfluorotridecanoic acid	PFTriDA	$C_{12}F_{25}COOH$
Perfluorotetradecanoic acid	PFTetA	$C_{13}F_{27}COOH$
Perfluoropentanedecanoic acid	PFPA	$C_{14}F_{29}COOH$
Perfluorohexanedecanoic acid	PFHxDA	$C_{15}F_{31}COOH$
Perfluoroalkyl Sulfonic Acids (PFSAs)		
Perfluorobutane sulfonic acid	PFBS	$C_4F_9SO_3H$
Perfluorohexane sulfonic acid	PFHxS	$C_6F_{13}SO_3H$
Perfluorooctane sulfonic acid	PFOS	$C_8F_{15}SO_3H$
Perfluorodecane sulfonic acid	PFDS	$C_{10}F_{21}SO_3H$

Table 1.2 Summary of PFOS and PFOA properties, (US EPA, 2014).

Property	**PFOS**	**PFOA**
Water solubility at 25°C [mg L^{-1}]	550 to 570	9.5×10^{3}
Henry's law constant [atm m^3 mol^{-1}]	3.05×10^{-9}	Not measurable
Half-life, water [years]	> 41	> 92
pK_a	-3.27	2.50

Table 1.3 Summary of global drinking water guidelines for PFOS and PFOA.

Region	Compound	Maximum, ng L^{-1}	Source
North America			
United States	PFOS+PFOA	70	(US EPA, 2016)
Minnesota	PFOS+PFOA	300	(US EPA, 2014)
New Jersey	PFOA	40	
North Carolina	PFOA	2,000	
Canada	PFOS	200	(Health Canada, 2016a)
	PFOA	600	(Health Canada, 2016b)
International			
The Netherlands	PFOS	0.65	(Moermond et al., 2010)
Germany	PFOS+PFOA	100	(DWC, 2006)

Chapter 2

Influence of Temperature, pH Condition and Dosage on the Removal of PFOS in the Presence of Granular Zerovalent Iron

2.1 Executive Summary

Perfluorooctane sulfonic acid (PFOS) is a persistent organic pollutant found in groundwater environments. Successful removal of PFOS using treatments applicable for the subsurface remains a challenge. PFOS removal over a 14-day period, when reacted with granular zerovalent iron (ZVI) under anaerobic conditions, was measured as a function of initial pH (pH_i 2.0 and 6.6), temperature (room temperature and 60°C) and ZVI dosage (179 and 1792 mM). PFOS removal from the aqueous phase after the 14-day treatment period ranged from 11 to 92%. Greatest PFOS removal was achieved under low initial pH, high temperature, and high ZVI dosage conditions. A mass balance of PFOS removal was performed to evaluate removal mechanisms. PFOS removal by sorption at the 14-day treatment period ranged from 4 to 48%. Iron oxides likely play a significant role in PFOS removal. Neither F^- nor short-chain PFSAs were observed, and as a consequence, PFOS degradation cannot be confirmed. PFOS removal is achieved in the presence of ZVI, however, more research is needed to understand PFOS removal mechanisms and complete the unknown portion of the mass balance.

2.2 Introduction

Perfluoroalkyl substances (PFASs) are a diverse group of persistent organic pollutants that are used in a wide variety of industrial applications and are detected ubiquitously in the environment (Buck et al., 2011). Perfluorooctane sulfonic acid (PFOS) is a PFAS commonly detected in the environment and consists of a hydrophobic chain of eight carbons saturated with fluorine, and a hydrophilic sulfonate head group which enhances its solubility in water (Ahrens, 2011). Fluorine is the most electronegative element and when combined with carbon it creates the strongest bond

known in organic chemistry. The strength of the C-F bond results in extreme thermal and chemical stability of PFOS making it useful for a variety of industrial applications (Kissa, 1994). PFOS from metal plating, textile facilities, manufacturing and aqueous film-forming foams (AFFFs) sources is released into the environment and reaches groundwater (Liu et al., 2015; Xie et al., 2013). The breakdown of fluorotelomer sulfonates in the environment can also contribute to the presence of PFOS in the environment (Houtz et al., 2013). PFOS is included as an Annex B substance in the Stockholm Convention on persistent organic pollutants in 2009 due to its persistence, bioaccumulation and adverse effects to wildlife and human health (Gewurtz et al., 2013; Kannan, 2011). The United States Environmental Protection Agency has set provisional health advisories of PFOS combined with perfluorooctanoic acid (PFOA) in drinking water of 70 ng L^{-1} (US EPA, 2016). PFOS is found at concentrations up to 2300 μg L^{-1} in impacted groundwater in the United States, well above the recommended health advisory limit (Rayne & Forest, 2009).

To date, PFOS is not found to degrade in the environment naturally and is not effectively removed by wastewater treatment plants (Arvaniti et al., 2012; Key et al., 1998). PFOS removal by sorption materials using powdered activated carbon, granular activated carbon, reverse osmosis, inorganic oxides, layered hydroxides and magnetite nanoparticles indicate variable effectiveness (Gong et al., 2016; Hansen et al., 2010; Hu et al., 2017; Sun et al., 2016; Tang et al., 2006). Advanced oxidation processes are fairly ineffective in the destruction of PFOS (Schröder & Meesters, 2005). PFOS is marginally removed in the presence of persulfate activated by heat, ultraviolet light, iron, and ultrasound as well as heat-activated permanganate, but is more resistant than its carboxylate counterpart perfluorooctanoic acid (PFOA) (Liu et al., 2012b; Park et al., 2016; Yang et al., 2013).

Comparatively few studies evaluate PFOS removal using reductive mechanisms.

Ochoa-Herrera et al. (2008), observed partial removal of PFOS in the presence of Ti(III)-citrate with a vitamin B_{12} catalyst under temperatures of 70°C and highly alkaline pH after a 7-day period. Jin & Zhang (2015), examined the application of hydrated electrons in an anoxic alkaline solution under vacuum ultraviolet light resulting in complete PFOS defluorination. Hori et al. (2006), achieved up to 51% PFOS defluorination using zerovalent iron in subcritical water (350°C) and high pressure (23 MPa) conditions after 6 hours of exposure. While the above studies demonstrate there are options for PFOS removal, many require extreme operating conditions and may be costly and difficult to apply in the subsurface. Magnesium amino-clay coated zerovalent iron nanoparticles under room temperature and initial pH 3 conditions removes greater than 90% of PFOS after 1 hour of exposure (Arvaniti et al., 2015). Greater than 30% of PFOS is removed after 6 days in the presence of palladium-coated zerovalent iron nanoparticles (PdnZVI) under initial pH 3.6 and 70°C conditions (Park et al., 2017). Both studies demonstrate promise in terms of potential subsurface application but disagree in terms of the effectiveness of temperature.

Granular zerovalent iron (ZVI) is a non-toxic, abundant and relatively inexpensive reductive material that requires little maintenance, and can be used in permeable reactive barriers as a cost-effective technology for *in situ* remediation of groundwater systems or in flow-through reactors for wastewater treatment (Fu et al., 2014; Prasad et al., 2011). The iron oxide shell acts as a site for sorption of contaminants, while the core acts as an electron donor to promote reductive reactions (Li et al., 2006). A variety of contaminants can be removed in the presence of ZVI, namely chlorinated organic compounds which have a similar bond strength to fluorinated organic compounds (Fu et al., 2014; Kissa, 1994).

Few studies to date have investigated the application of ZVI for the degradation of PFOS that would be applicable for subsurface applications, while no studies pub-

licly available have examined the removal of PFOS in the presence of granular ZVI. Thus, the main objective of this study was to investigate the removal of PFOS in the presence of granular ZVI under various conditions. The secondary objective of this study was to assess the removal mechanism through completion of a PFOS mass balance. The influence of initial pH, temperature and ZVI dosage on PFOS removal was investigated. The removal mechanism was assessed through (i) analysis of released F^- ions in the aqueous solution and (ii) analysis of short-chain PFSA compounds in the aqueous solution, as well as (iii) extracted PFOS sorbed to the ZVI surface to construct a mass balance.

2.3 Materials and Methods

2.3.1 Chemicals and Reagents

Ultrapure water was provided by a Milli-Q system (EMD Millipore, 18.2 MΩ·cm at 25°C). Argon gas was ultrahigh purity from Praxair Inc. (Mississauga, Ontario, Canada). Iron aggregate (87-93%, Connelly GPM Inc.) was sieved to achieve a grain size between 0.25 and 1.19 mm and washed using hydrochloric acid to remove accumulated oxide coatings (HCl, 36.5-38%, J.T. Baker). PFOS ($C_8F_{17}SO_3H$, $\geq$ 98%) was obtained from Sigma Aldrich (Mississauga, Ontario, Canada). Sodium perfluoro-1-heptanesulfonate (PFHpS, $C_7F_{15}SO_3Na$), sodium perfluoro-1-hexanesulfonate (PFHxS, $C_6F_{13}SO_3H$), potassium perfluoro-1-butanesulfonate (PFBS, $C_4F_9SO_3H$) and isotopically labeled standards [$^{13}C_4$]-PFOS (MPFOS, $C_8F_{17}SO_3Na$, $\geq$ 99%) and [^{18}O]-PFHxS (MPFHxS, $C_6F_{13}SO_3Na$, $\geq$ 94%) for use as internal standards were purchased from Wellington Laboratories (Guelph, Ontario, Canada). High-performance liquid chromatography tandem mass spectrometry (HPLC-MS/MS) analysis used methanol ($\geq$ 99.9%, HPLC-MS grade, Mississauga, Canada) and ammonium acetate (HPLC grade,

Oakville, Canada) purchased from Sigma-Aldrich. PFOS extracted from the surface of ZVI to investigate sorption used glacial acetic acid (CH_3COOH, 99.7%, Fisher Scientific) and methanol ($\geq$ 99.9%, HPLC-MS grade, Sigma-Aldrich). Anion standard used for fluoride and acetate calibration was purchased from Inorganic Ventures (Christiansburg, Virginia, USA). Sodium fluoride (NaF, $\geq$ 99%, Anachemia) was used to spike fluoride controls. Iron phases from the iron surface were extracted using hydrochloric acid, sodium acetate ($C_2H_3NaO_2$, 98%, Sigma-Aldrich), sodium bicarbonate ($NaHCO_3$, $\geq$ 99.7%, BDH) and sodium ascorbate ($C_6H_7NaO_6$, $\geq$ 99%, Sigma Aldrich). Analysis of the valence state of the solid iron used ferric ammonium sulfate dodecahydrate ($NH_4Fe(SO_4)_2{\cdot}12H_2O$, > 98.5%, EMD), sodium acetate ($C_2H_3NaO_2$, $\geq$ 99%, Sigma-Aldrich), glacial acetic acid (CH_3COOH, $\geq$ 99.7%, Fisher Scientific), ferrozine ($C_{20}H_{13}NaO_6H_2O$, 95%, J.T. Baker) and hydroxylamine hydrochloride (H_3NHCl, 99.8%, Fisher Scientific).

2.3.2 Batch Experimental Systems

Batch experiments were performed to investigate PFOS removal under multiple controlled reaction conditions (Figure 2.1). Connelly ZVI was washed using 1.2 M HCl and decanted seven times, then transferred into an anaerobic glovebox (Coy Laboratories). To remove residual acid, the ZVI was rinsed with Argon-purged ultrapure water three times. Individual polypropylene centrifuge tube reactors were transferred into an anaerobic glovebox, volumetrically filled with Argon-purged ultrapure water and spiked with PFOS from a methanol stock for a concentration of 19 $\pm$ 5 μM. The effects of initial pH were examined by preparing sets of reactors with initial uncontrolled pH (pH_i = 6.6 $\pm$ 0.4, labeled as pH_i 6.6) or initial pH to 2 $\pm$ 0.3 (labeled as pH_i 2.0) adjusted with HCl. The role of ZVI dosage was examined by adding two different quantities of ZVI, with concentrations of either 179 or 1792 mM. The

molar ratio of ZVI:PFOS was either 8956 or 89557. ZVI was added by mass to each reactor inside the anaerobic glovebox. Sealed reactors were placed in glass jars filled with Argon-purged water to ensure anaerobic conditions were maintained outside of the glovebox. The influence of temperature was controlled by placing samples either at room temperature ($\backsim$22°C) or at 60 $\pm$ 1.0°C using a microcontrolled water bath on a shaker at 10 rpm for the treatment period of 13.9 $\pm$ 0.2 days. In each batch experiment, 20% of samples were performed in duplicate reactors.

To assess the presence of PFOS in the water, ultrapure water blanks were included. ZVI only controls assessed any PFOS contribution from ZVI. PFOS in ultrapure water controls were used to quantify the initial concentration C_0 as a reference point to assess removal. Fluoride and ZVI in ultrapure water assessed any removal of F^- from the aqueous phase. The fluoride spike of 340 μM simulated the maximum potential defluorination of the initial PFOS concentration. Controls were performed with each batch test under the same initial pH and temperature conditions.

Treatment samples were collected at 0.5, 1, 2, 4, 7, 10 and 14 days and controls collected at 0.5 or 2, 7 and 14 days. Reactors were brought into the glovebox and aqueous aliquots were used to measure pH and Eh conditions. Reactors were tightly capped with parafilm, removed from the glovebox, and centrifuged at 3500 rpm for 15 minutes. Centrifuged reactors were brought back into the glovebox and the aqueous supernatant decanted from the solid slurry into separate 50 mL polypropylene centrifuge tubes and both phases were stored at $\leq$ 4°C until analysis.

2.3.3 Analytical Methods

Aqueous supernatant samples were equilibrated to room temperature, serially diluted by a factor of 5000 with ultrapure water by mass and spiked with an internal standard mixture which contained 20 μg L^{-1} [^{13}C]-PFOS and [^{18}O]-PFHxS for a

total of 20 mL diluted sample. Diluted samples were then passed through solid phase extraction (SPE) cartridges by gravity and concentrated by a factor of 10 (Oasis HLB 3 cc 60 mg, Waters Corp., Mississauga, Canada). The cartridges were preconditioned with 2 mL methanol (HPLC grade), washed with 2 mL ultrapure water, loaded with 20 mL diluted sample, washed with 2 mL ultrapure water, vacuum dried for 30 seconds and eluted with 2 mL methanol. The 2 mL PFAS extracts were collected in 5 mL polypropylene Eppendorf tubes and stored at ≤ 4°C.

The concentrations of selected PFASs in methanol extracts were determined by HPLC (1290 HPLC, Agilent Technologies, Mississauga, Canada) followed by MS/MS (6460 QQQ, Agilent Technologies, Mississauga, Canada) equipped with an electrospray interface operated in negative mode. Methanol extracts were equilibrated to room temperature prior to analysis. A 10 μL aliquot of the methanol PFAS extract was injected and separated on a Pursuit XRS Ultra column (2.8 μm i.d., 50 mm $\times$ 2 mm) (Agilent, Mississauga, Canada) maintained at 55°C for quantitative analysis. The mobile phase consisted of 2 mM ammonium acetate in water (Phase A) and in methanol (Phase B) with a flow rate of 0.5 mL min^{-1}. Gradient conditions can be found in Table 2.1. Ions were acquired in multiple reaction monitoring mode with a dwell time of 30 ms and cell accelerator voltage of 4 V. Instrument conditions and monitored parent and product ions can be found in Tables 2.2 and 2.3, respectively. A fresh calibration curve for a combined mixture of all PFASs was created for each batch of analyses with each compound calibration curve linear in the range of 0.5 to 30 μg L^{-1} ($R^2 > 0.99$). Each set of analyses ran for a maximum of 24 hours and a methanol blank was analyzed between each sample to prevent accumulation of PFASs on the column. The HPLC tubing was cleaned with a 50:50 (v/v) methanol:acetonitrile mixture overnight and the column with methanol for two hours prior to analysis to remove any residual PFAS build-up. Internal standard recovery was assessed for all

samples and the analysis was accepted if recovery was between 70 and 130%. Each sample was analyzed at least twice and on separate days. The method detection limits (MDLs) of PFOS, PFHpS, PFHxS, and PFBS were 350, 90, 170 and 100 ng L^{-1}, respectively.

PFOS sorption to the ZVI surface as a possible removal mechanism was examined by extracting PFOS from the surface of ZVI grains into an aqueous phase according to the method described in Arvaniti et al. (2014) with some modifications. An aliquot of 0.1 g of ZVI was dried overnight and transferred to a 15 mL polypropylene centrifuge tube. Liquid-solid extraction was performed by adding 7.5 mL of 1% (v/v) acetic acid in water and 1.5 mL methanol to the dried ZVI. The samples were vortexed for 1 minute, sonicated for 15 minutes and centrifuged at 3500 rpm for 15 minutes. The process was repeated two more times for each sample with 7.5 mL of 1% (v/v) acetic acid in water added. The supernatant was collected after each extraction process in a separate polypropylene centrifuge tube and stored at $\leq 4°C$. Each sample was extracted in duplicate. Samples were diluted by a factor of 200 and passed through SPE prior to HPLC-MS/MS analysis.

The concentrations of fluoride in the aqueous supernatant samples were determined using ion chromatography (Dionex ICS-5000$^+$ DCS). Aqueous samples and standards were filtered with a 0.2 μm filter (PTFE, Pall Acrodisc) the day of analysis. A 10 μL aliquot of each sample was injected onto a column (IonPac AS18 2 $\times$ 50 mm) with a KOH eluent at a 0.25 mL min^{-1} flow rate. Gradient conditions can be found in Table 2.4. Acetate was included in the analysis due to the proximity of elution to fluoride in the presence of ZVI as found by Arvaniti et al. (2015). Fluoride and acetate were calibrated with linearity in the range of 80 to 2000, and 200 to 12500 μg L^{-1}, respectively. The MDLs of fluoride and acetate were 4 and 18 μg L^{-1}, respectively.

Analysis of the ZVI grains was performed to provide information regarding the oxidation state of iron on the grain surfaces throughout the treatment period. A dilute acid iron extraction method was prepared as described in Heron et al. (1994), using 0.5 M hydrochloric acid in solution to extract poorly crystalline phases and poorly adsorbed phases of iron. An ascorbate buffer solution was prepared as described in Amirbahman et al. (1998), using a sodium ascorbate, sodium citrate and sodium bicarbonate buffer to extract poorly crystalline and amorphous oxyhydroxide phases at a higher pH. The reagents and method for the Ferrozine spectrophotometric method were prepared as described in Gibbs (1979). Ferrozine is added to each sample to create a purple colour in the presence of Fe(II) for colourimetric measurements. Hydroxylamine hydrochloride is added to samples to reduce Fe(III) to Fe(II) to allow calculation of total iron concentration. By analyzing extracts both with and without the reductant, concentrations of both Fe(II) and Fe(III) in each sample can be determined. An aliquot of an acetic acid buffer made of sodium acetate and glacial acetic acid was used to bring the pH within 3 to 5 for aqueous Fe(II). Each sample was extracted in duplicate and Fe(II) was analyzed using a Hach DR 2800 at 562 nm wavelength after being calibrated to linearity within 50 to 800 μg L^{-1}.

2.3.4 Calculations

Statistical significance between the influences of ZVI dosage, temperature and initial pH at the end time point was calculated using one-way analysis of variance. A p-value of 0.05 was used to assess statistically significant differences between the groups.

The extent of defluorination was calculated to determine the degree of mineral-

ization of PFOS based on measured fluoride concentration in each sample:

$$Theoretical F^{-}, mgL^{-1} = \frac{input PFOS mg}{L} \times \frac{mmol PFOS}{500.13 mg} \times \frac{17 mmol F^{-}}{mmol PFOS} \times \frac{19 mg F^{-}}{mmol} \quad (2.1)$$

$$Defluorination, \% = \frac{measured F^{-}, mgL^{-1}}{theoretical F^{-}, mgL^{-1}} \times 100\% \quad (2.2)$$

2.4 Results and Discussion

2.4.1 Effect of ZVI Dosage on PFOS Removal

The effect of the three granular ZVI dosages on PFOS removal was investigated under a combination of all pH and temperature conditions (Figure 2.2). At 14 days at 60°C and pH_i 6.6 conditions, there was 28 and 63% of PFOS removed in the presence of 179 and 1792 mM ZVI, respectively (Figure 2.2A). As ZVI dosage was increased, the degree of PFOS removed also increased. At 60°C and pH_i 2.0 at 14 days, there was 78 and 92% of initial PFOS removed in the presence of 179 and 1792 mM ZVI, respectively (Figure 2.2B). Similar to pH_i 6.6 conditions, the increase in ZVI dosage under pH_i 2.0 led to a proportional increase in PFOS removed. At room temperature and pH_i 6.6 conditions at 14 days, there was 11 and 34% PFOS removed in the presence of 179 and 1792 mM ZVI, respectively (Figure 2.2C). At 14 days at room temperature and pH_i 2.0 conditions, days there was 56 and 58% PFOS removal in the presence of 179 and 1792 mM ZVI, respectively (Figure 2.2D). Under pH_i 6.6 there was a 23% increase in PFOS removal in the presence of a greater proportion of ZVI, while there was only a 2% increase in PFOS removal under pH_i 2.0 conditions.

Single-factor ANOVA analysis was conducted between the ZVI dosages and a significant statistical difference was found ($p \leq 0.0476$) for PFOS removal under all conditions except for under pH_i 2.0 and room temperature conditions. It is possible

that the difference in the ZVI:PFOS molar ratio may need to be larger than a factor of 9 to be statistically significant under all conditions. Findings are in line with Arvaniti et al. (2015), where the increased dosage of zerovalent iron nanoparticles enhanced PFOS removal due to greater surface available for reaction.

2.4.2 Effect of Initial pH on PFOS Removal

The pH of pH_i 6.6 rose to pH 7.0 $\pm$ 0.8 after the first sampling time and for the remainder of the treatment period (Figure A.1). The pH of pH_i 2.0 rose to 6.1 $\pm$ 1.1 within 4 days for the remainder of the treatment period (Figure A.2). Any differences in PFOS removal due to pH condition were likely due to differences in initial pH, as the pH of both pH_i 2.0 and pH_i 6.6 were within 1.2 units for the remainder of the treatment period after 4 days.

The effects of pH_i 2.0 and pH_i 6.6 on PFOS removal were studied at all ZVI dosages and temperature conditions (Figure 2.3). At 14 days under 60°C and 179 mM ZVI at 14 days, 78 and 28% of PFOS was removed under pH_i 2.0 and pH_i 6.6, respectively (Figure 2.3A). At 14 days under 60°C and 1792 mM ZVI, 92 and 63% of PFOS were removed under $_i$ 2.0 and pH_i 6.6, respectively (Figure 2.3B). Under all ZVI dosages at 60°C, PFOS is removed to a greater degree under pH_i 2.0 compared to pH_i 6.6 conditions. At 14 days at room temperature and 179 mM ZVI, 56 and 11% of PFOS were removed under pH_i 2.0 and pH_i 6.6 conditions, respectively (Figure 2.3C). At room temperature and 1792 mM ZVI at 14 days, 58 and 34% of PFOS was removed when under pH_i 2.0 and pH_i 6.6 conditions, respectively (Figure 2.3D). Similar to 60°C under all ZVI dosages, at room temperature PFOS is removed to a greater degree under pH_i 2.0 compared to pH_i 6.6 conditions.

Statistically significant differences ($p \leq 0.0191$) in PFOS removal were observed between pH_i 2.0 and pH_i 6.6 under all temperature and ZVI dosage conditions. The

finding that lower initial pH results in greater PFOS removal by ZVI is consistent with findings by Arvaniti et al. (2015) and Fang et al. (2011). In the presence of water, the ZVI surface is corroded according to:

$$Fe(0) + 2H_2O \rightarrow Fe(II) + H_2 + 2OH^- \tag{2.3}$$

At lower pH, corrosion of the ZVI surface is enhanced in the presence H^+ ions by the following reaction:

$$Fe(0) + 2H^+ \rightarrow Fe(II) + H_2 \tag{2.4}$$

As ZVI is oxidized to Fe(II), electrons are released and are available to react with the highly electronegative fluorine atoms (E_0 = 3.6 V), where RF represents fluorine bonded to a carbon of the PFAS chain (Li et al., 2006; Vecitis et al., 2009):

$$Fe(0) \rightarrow Fe(II) + 2e^- \tag{2.5}$$

$$RF + H^+ + 2e^- \rightarrow RH + F^- \tag{2.6}$$

Increased surface corrosion of ZVI at low pH increases the degree of iron oxides present on the surface, enhancing PFOS sorption to the ZVI surface (Gao & Chorover, 2012). At higher pH (> 5), PFOS removal is inhibited by surface passivation of ZVI by secondary oxide precipitates and greater aggregation of ZVI, reducing surface area available for reaction (Khan et al., 2017). ZVI exhibits a positive charge below its point of zero charge of 7.8 which may further enhance the attraction of anionic PFOS (pK_a = -3.27) through electrostatic interaction (Gao & Chorover, 2012; Hu et al., 2017; Kanel et al., 2005). The pH of pH_i 2.0 increased to pH = 6.1 $\pm$ 1.1 after 4 days and is within a 1.2 pH unit difference as the pH_i 6.6 treatment samples (Figures A.1, A.2), suggesting that enhanced PFOS interaction with the corroded

ZVI surface occurs within the 4-day time frame. PFOS removal was enhanced under lower pH conditions likely due to a greater presence of iron oxides and electrostatic interaction with the ZVI surface (Johnson et al., 2007). PFOS removal under pH_i 6.6 was observed but to a lesser extent than pH_i 2.0, likely due to a lower abundance of iron oxides available for sorption and a smaller charge difference between the ZVI surface and PFOS functional group, reducing electrostatic interaction.

2.4.3 Effect of Temperature on PFOS Removal

The effect of two constantly held temperatures on PFOS removal was evaluated under all ZVI dosage and pH conditions (Figure 2.4). At 14 days under 179 mM ZVI and pH_i 2.0 conditions, 78 and 56% of PFOS was removed at 60°C and room temperature, respectively (Figure 2.4A). At 14 days under 1792 mM ZVI and pH_i 2.0 at 14 days, 92 and 58% of PFOS was removed at 60°C and room temperature, respectively (Figure 2.4B). Under pH_i 2.0 and all ZVI dosage conditions, PFOS removal is greater at 60°C compared to room temperature. At 14 days under 179 mM ZVI and pH_i 6.6 conditions, 28 and 11% of PFOS was removed at 60°C and room temperature, respectively (Figure 2.4C). Under 1792 mM ZVI and pH_i 6.6 at 14 days, 63 and 34% of PFOS was removed at 60°C and room temperature, respectively (Figure 2.4D). Under pH_i 6.6 and all ZVI dosage conditions, PFOS removal is greater at 60°C compared to room temperature.

There were statistically significant differences ($p \leq 0.0297$) in PFOS removal between room temperature and 60°C conditions under a ZVI dosage of 1792 mM, but not under 179 mM ZVI. Enhanced PFOS removal at higher temperatures only under the higher ZVI dosage suggests that the role of temperature in PFOS removal is related to the abundance of ZVI. It is likely PFOS removal is endothermic and activation energies are reduced under higher temperatures (Boparai et al., 2011).

PFOS removed by sorption was generally not enhanced under higher temperature conditions compared to room temperature, suggesting increased PFOS removal under higher temperatures may be caused by an alternative mechanism. Park et al. (2017) also found greater PFOS removal at higher temperatures. The finding that higher temperature enhances PFOS removal is in line with other studies using uncoated ZVI which report enhanced removal of PFOS, organochlorine pesticides and nitrate under higher temperatures (Ahn et al., 2008; Hori et al., 2006; Saha & Sinha, 2015).

2.4.4 Mass Balance

A mass balance was performed under all conditions at multiple time points to assess possible PFOS removal mechanisms (Figure 2.5, 2.6). The mass balance is represented as a fraction of the initial PFOS concentration and all measurements were adjusted to molar PFOS equivalents. The mass balance presents remaining aqueous PFOS, aqueous fluoride, PFOS on the surface of ZVI, aqueous PFSA short-chains and any remaining fraction as unknown at their respective sampling time point. Fluoride concentration was analyzed to assess the degree of cleavage of the C-F bond, as it would indicate PFOS degradation (Hori et al., 2006). The concentration of F^- in all samples was below the MDL, with defluorination less than 0.5% of the initial PFOS input under all conditions (Figure 2.7, 2.8). A portion of the initial aqueous fluoride in the control containing fluoride and ZVI only was removed in the presence of iron, likely due to sorption to iron hydroxides (Figure 2.7, 2.8) (Sujana et al., 2009). Removal of aqueous fluoride through sorption to iron hydroxides could potentially represent F^- release from C-F bond breakage, of up to 11% and 50% of maximum PFOS defluorination under pH_i 6.6 and pH_i 2.0 conditions, respectively. Thus, reductive defluorination of PFOS could be higher than it appears as there may

be aqueous F^- removed in the presence of ZVI.

Another expected by-product of PFOS degradation would be the presence of PFSA short-chains, which represented a maximum of 6% of the initial PFOS input with no indication of increasing concentrations throughout the treatment period under any condition (Figure 2.9, 2.10). No PFSA short chains were detected above the MDLs for PFBS, PFHxS or PFHpS in the aqueous phase from the ZVI surface extraction, indicating there was little or no sorption. PFSA short chain concentrations were similar to the input PFOS controls, suggesting their presence may not be due to generation from PFOS degradation, but present in background concentrations.

The removal of PFOS by sorption onto the ZVI surface was investigated through extraction of PFOS from the ZVI surface (Figure 2.11, 2.12). Sorption of PFOS at pH_i 6.6 was found to represent 4 and 34% of PFOS removed at 60°C and 9 and 17% at room temperature in the presence of 179 and 1792 mM ZVI at 14 days (Figure 2.11). Sorption of PFOS at pH_i 2.0 was found to represent 14 and 45% of PFOS removed at 60°C and 15 and 48% at room temperature in the presence of 179 and 1792 mM ZVI at 14 days (Figure 2.12). Regardless of pH or temperature conditions, sorption appeared to generally increase as ZVI dosage is increased, suggesting surface area plays a role in sorption behaviour. Removal of PFOS removal under pH_i 2.0 conditions was 6 to 31% greater compared to pH_i 6.6, suggesting the increased presence of iron oxides may also play a role (Eqn. 2.4). Sorption of PFOS to ZVI is in line with Hori et al. (2006), in which a large portion of PFOS was removed prior to heating in the presence of ZVI.

Samples of ZVI solids under 1792 mM ZVI concentration, 60°C, and pH_i 2.0 conditions were analyzed at three time points for the presence of Fe(II) and Fe(III) in the solid phase (Table 2.5). Fe(III) and Fe(II) concentrations in the ZVI grains increased over the duration of the experiment when extracted using the diluted acid buffer, sug-

gesting adsorbed and poorly crystalline phases of Fe(III) and Fe(II) increased over time. The ratio of Fe(III)/Fe(II) increased over time, suggesting the accumulation of Fe(III) phases increased at a greater rate than Fe(II). Fe(III) extracted from ZVI using the ascorbate buffer also increased over time, suggesting an increased presence of amorphous oxyhydroxides. Poorly crystalline and amorphous iron oxyhydroxides are products of iron corrosion (Eqn. 2.3, 2.4) (Manning et al., 2002). PFOS removal attributed to iron oxide sorption is observed in previous studies (Park et al., 2017; Wei et al., 2017).

ZVI has an inner oxide shell of Fe_3O_4 and an outer shell of Fe_2O_3 surrounding the reduced iron core, however, there is almost no electron transfer at the Fe_2O_3 interface (Figure 2.13) (Odziemkowski & Simpraga, 2004). Further corrosion of the iron surface must occur for the Fe_2O_3 shell to dissolve and allow PFOS interaction with the Fe_3O_4 surface for electron transfer to occur. Corrosion of iron oxides occurs via the following reactions in order to reach equilibrium with Eqn. 2.5 (Qin et al., 2004):

$$Fe_2O_3 + 6H^+ + 2e^- \rightarrow 2Fe(II) + 3H_2O \tag{2.7}$$

$$Fe_3O_4 + 8H^+ + 2e^- \rightarrow 3Fe(II) + 4H_2O \tag{2.8}$$

It is possible that within the duration of the treatment, corrosion of the oxide shell was insufficient to adequately dissolve the Fe_2O_3 shell and allow PFOS interaction with the Fe_3O_4 surface for electron transfer. Reductive defluorination may also take a longer period of time to occur than examined in this study, due to the high bond dissociation energies of the C-F bonds (Blotevogel et al., 2017).

While a portion of the mass balance (0 to 58%) remains unknown, PFOS is not volatile and the loss is likely due to degradation to an unknown intermediate product or was partially degraded and could not be detected due to F^- sorption to ZVI (Voogt

& Saez, 2006). Temperature likely plays a role in the unknown removal mechanism, as the unknown portion of the mass balance at the 14-day time point was 9 to 36% greater than under room temperature conditions. Park et al. (2017) performed a QTOF analysis of the aqueous nZVI and PFOS mixture which reveals potential adducts of PFOS-Fe complexes, especially with Fe(III), which were not analyzed in this study but could be present. Removal mechanisms of PFOS in the presence of ZVI can be complex as interaction with iron phases may change over time and may be highly dependent on pH conditions. PFOS intermediates and degradation products may also have interactions with the ZVI surface over time, limiting proper quantification of the amounts released.

2.5 Conclusions

Granular ZVI is a potential reactive material for removal of PFOS from aqueous solutions. Removal was most efficient under low initial pH under all conditions and higher temperatures under high ZVI dosages. PFOS removal was greater under high ZVI dosages and is likely related to the increase in PFOS removed by sorption. Sorption was enhanced under low pH conditions, possibly due to increased iron oxides produced by corrosion reactions over time. Low fluoride concentrations present suggest reductive defluorination may not be the primary removal mechanism, however, F^- may be underestimated due to sorption to ZVI surfaces. Further research is required to examine proper analytical techniques to quantify complexation of PFOS with iron phases and close the unknown portion of the mass balance.

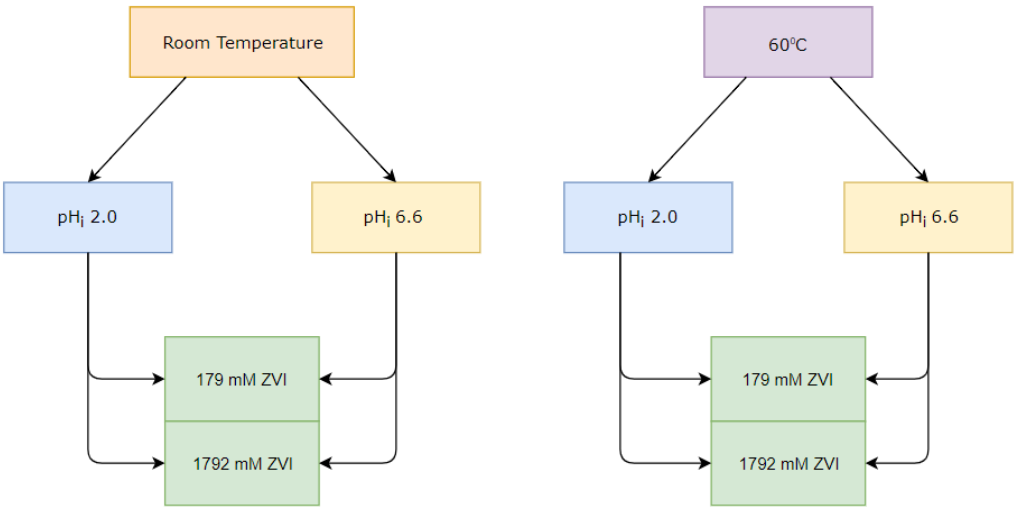

Figure 2.1 Outline of batch experiment variables for granular ZVI. A total of 8 different conditions were examined. Room temperature is approximately 22°C, while 60°C remained within 1°C. Uncontrolled pH was initially 6.6 ± 0.4 (pH$_i$ 6.6) then remained within 7.0 ± 0.8 throughout the duration of the experiment. Samples under pH$_i$ 2.0 started at 2.0 ± 0.3 and after 4 days remained within 6.1 ± 1.1.

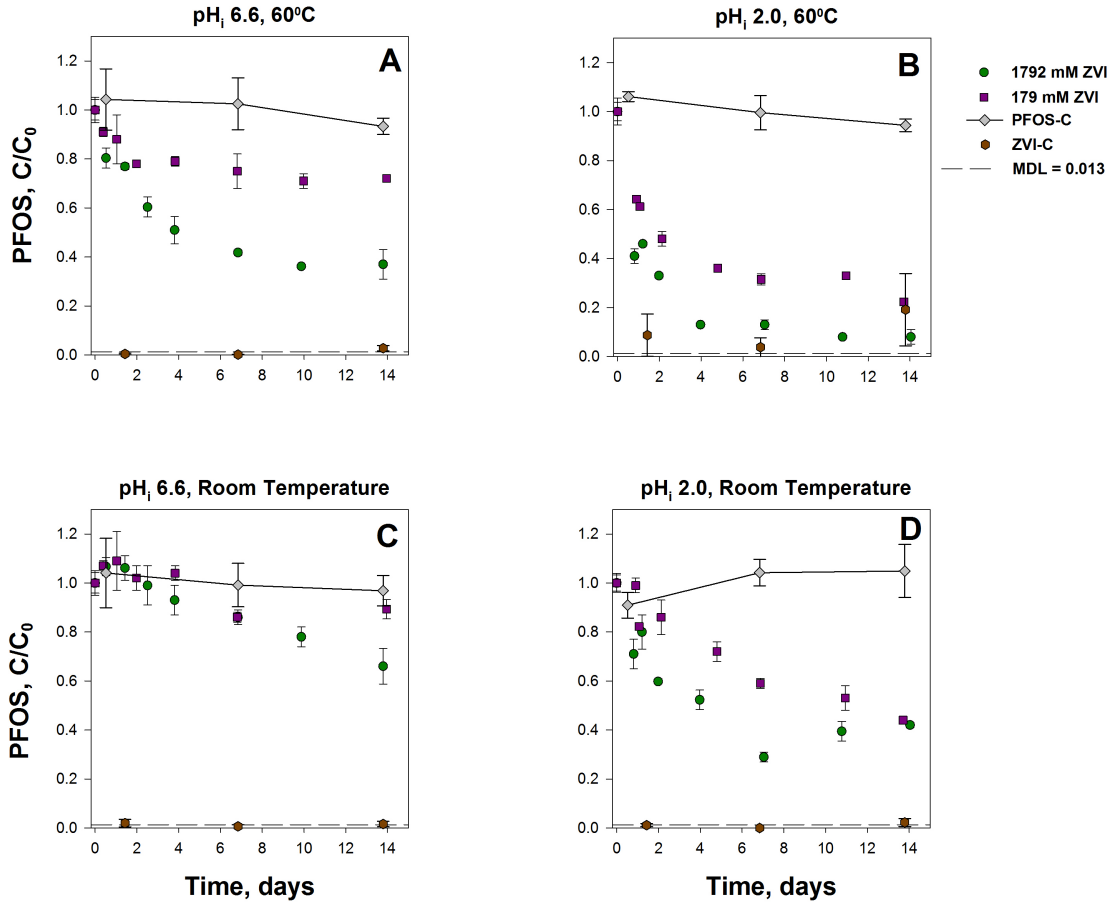

Figure 2.2 Summary of ZVI dosage on PFOS removal compared to initial PFOS concentrations. Figure 2.2A) pH$_i$ 6.6, 60°C, B) pH$_i$ 2.0, 60°C, C) pH$_i$ 6.6, room temperature, D) pH$_i$ 2.0, room temperature. Error bars represent the standard error from all possible sources of error (Table A.1).

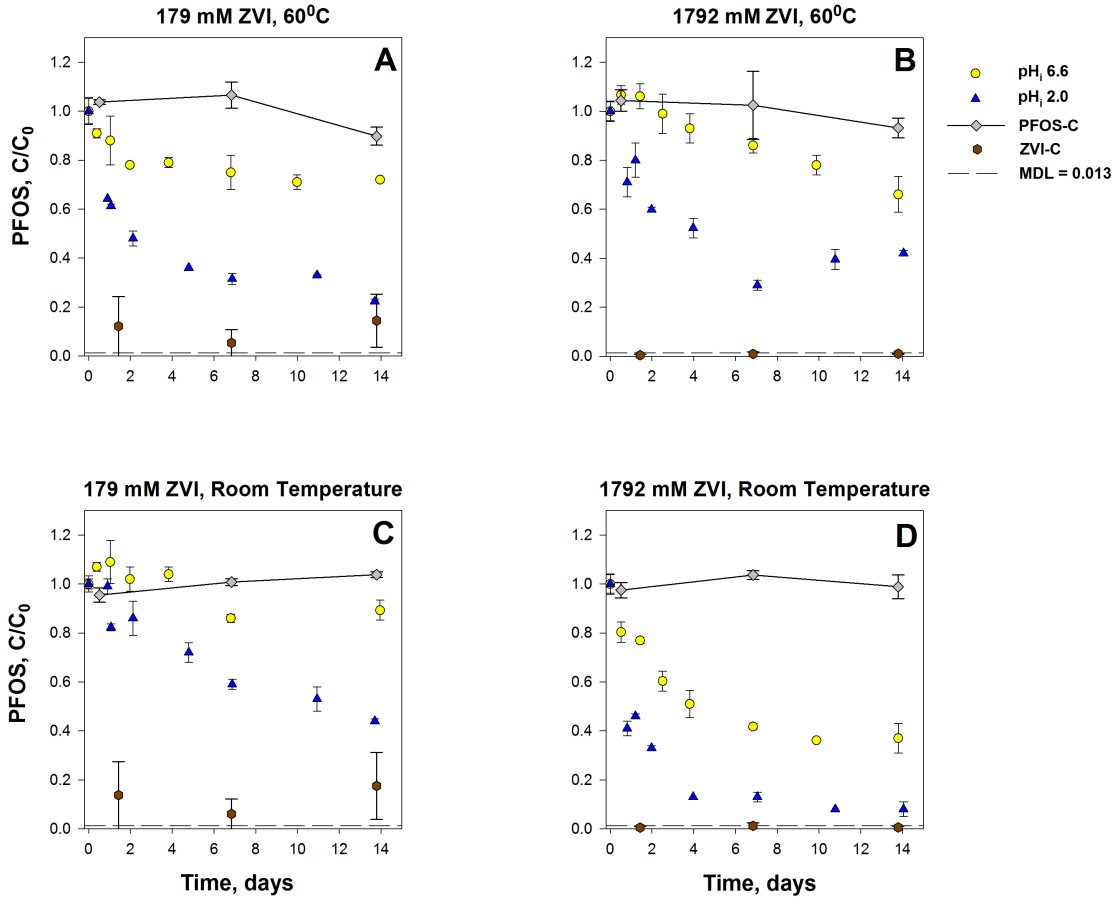

Figure 2.3 Summary of the influence of pH conditions on PFOS removal compared to initial PFOS concentration. Figure 2.3A) 179mM and 60°C, B) 1792 mM ZVI and 60°C, C) 179 mM and room temperature, D) 1792 mM ZVI and room temperature. Error bars represent the standard error from all possible sources of error (Table A.1).

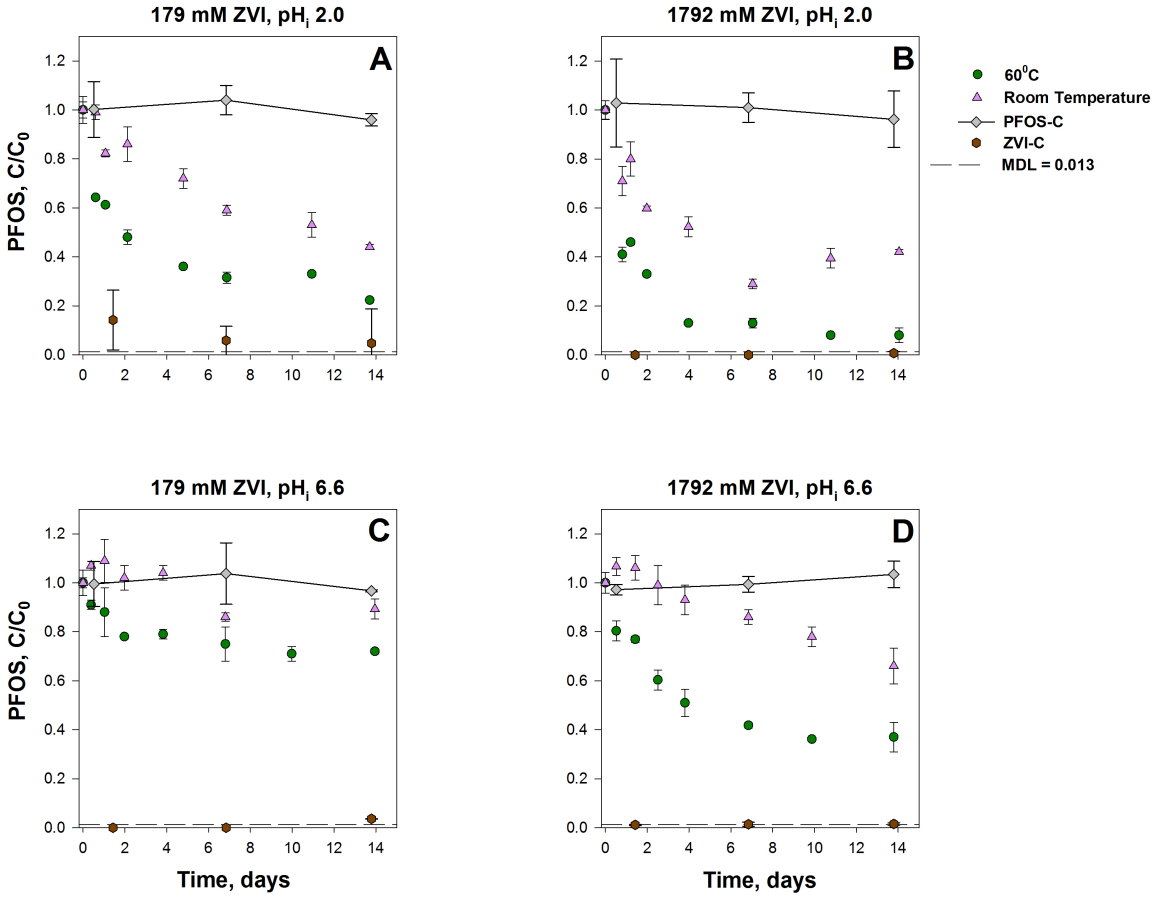

Figure 2.4 Summary of the influence of temperature on PFOS removal compared to initial PFOS concentration. Figure 2.4A) 179 mM ZVI and pH$_i$ 2.0, B) 1792 mM ZVI and pH$_i$ 2.0, C) 179 mM ZVI and pH$_i$ 6.6, D) 1792 mM ZVI and pH$_i$ 6.6. Error bars represent the standard error from all possible sources of error (Table A.1).

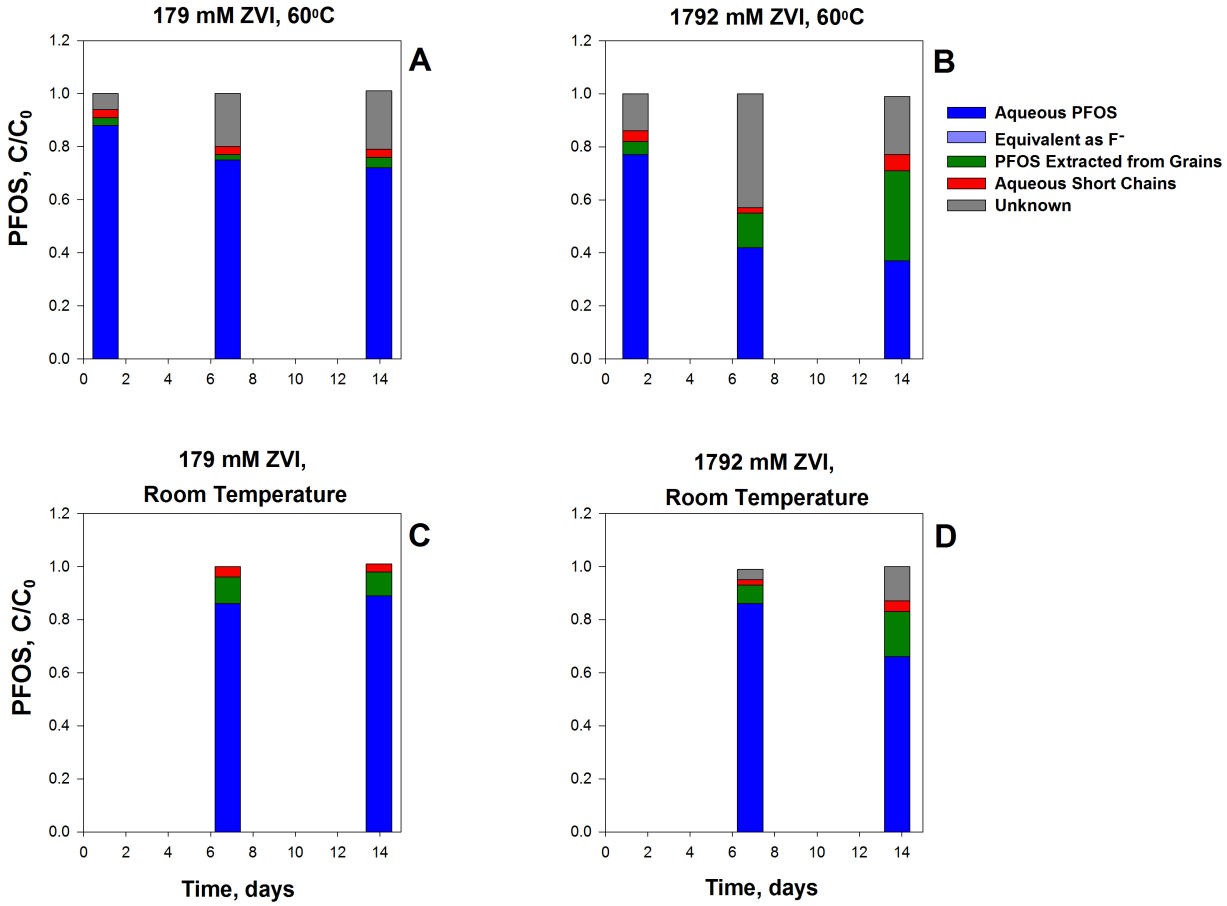

Figure 2.5 Mass balance of initial PFOS concentration under pH_i 6.6 conditions at select sampling points. Figure 2.5A) 179 mM ZVI and 60°C, B) 1792 mM ZVI and 60°C, C) 179 mM ZVI and room temperature, D) 1792 mM ZVI and room temperature. Only samples with all supporting analyses performed at the sampling time are shown in the mass balance.

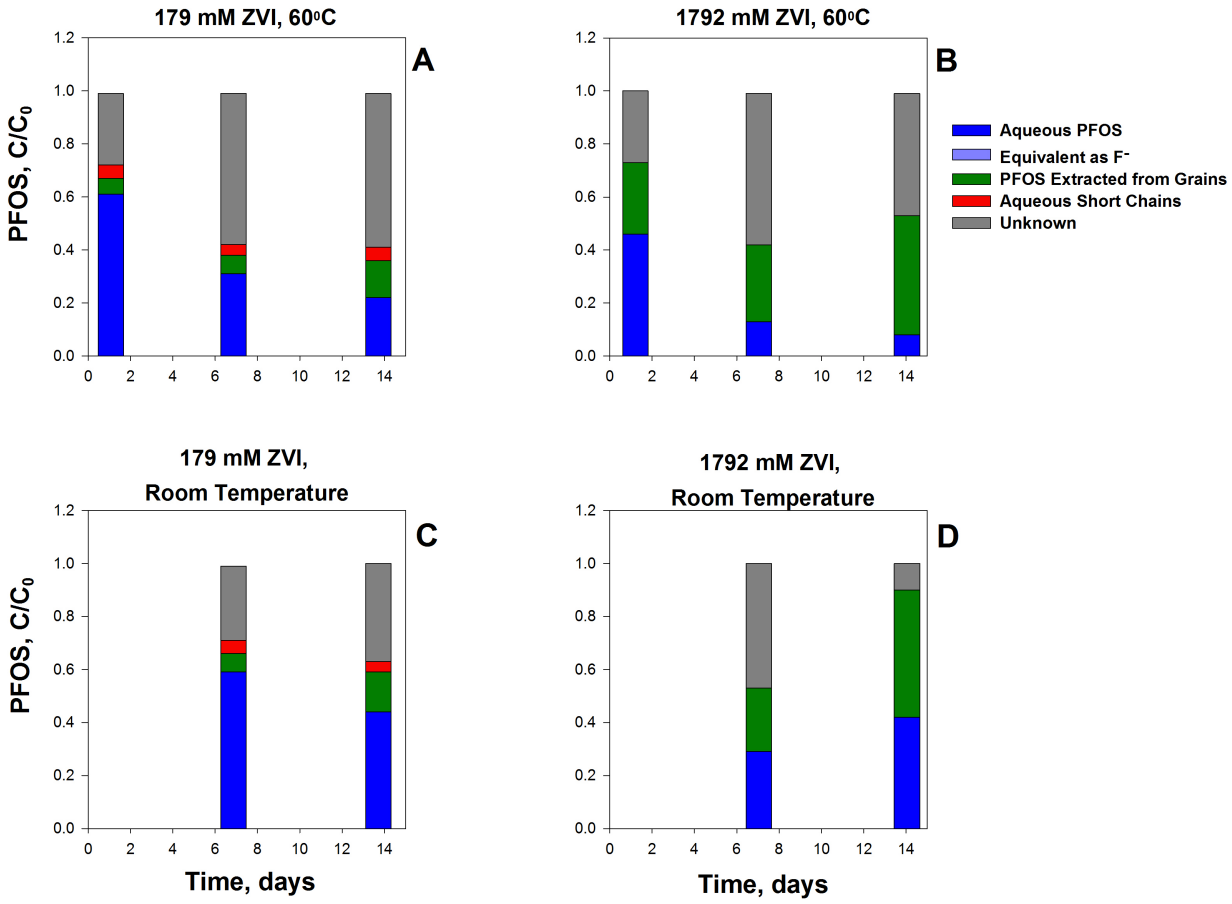

Figure 2.6 Mass balance of initial PFOS concentration under pH_i 2.0 conditions at select sampling points. Figure 2.6A) 179 mM ZVI and 60°C, B) 1792 mM ZVI and 60°C, C) 179 mM ZVI and room temperature, D) 1792 mM ZVI and room temperature. Only samples with all supporting analyses performed at the sampling time are shown in the mass balance.

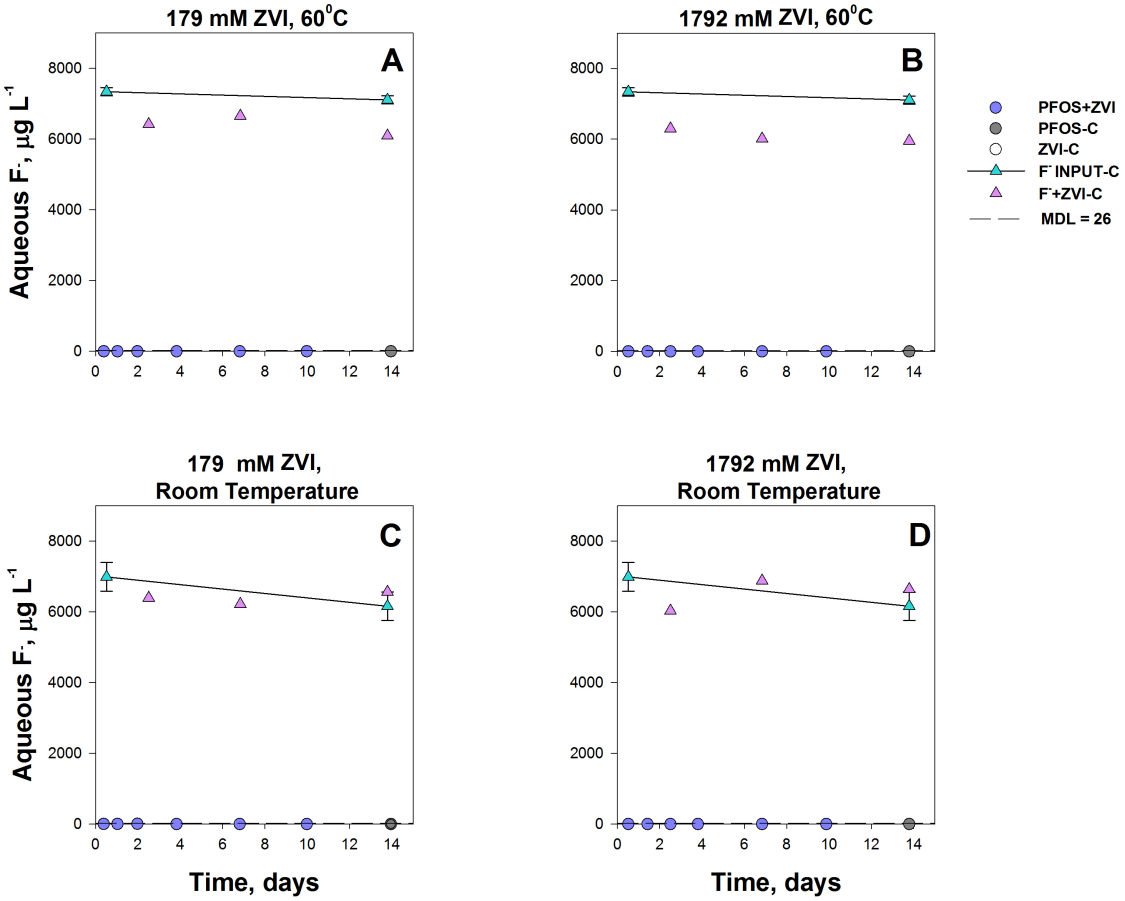

Figure 2.7 Summary of aqueous fluoride concentrations under pH_i 6.6 conditions. Figure 2.7A) 179 mM ZVI and 60°C, B) 1792 mM ZVI and 60°C, C) 179 mM ZVI and room temperature, D) 1792 mM ZVI and room temperature.

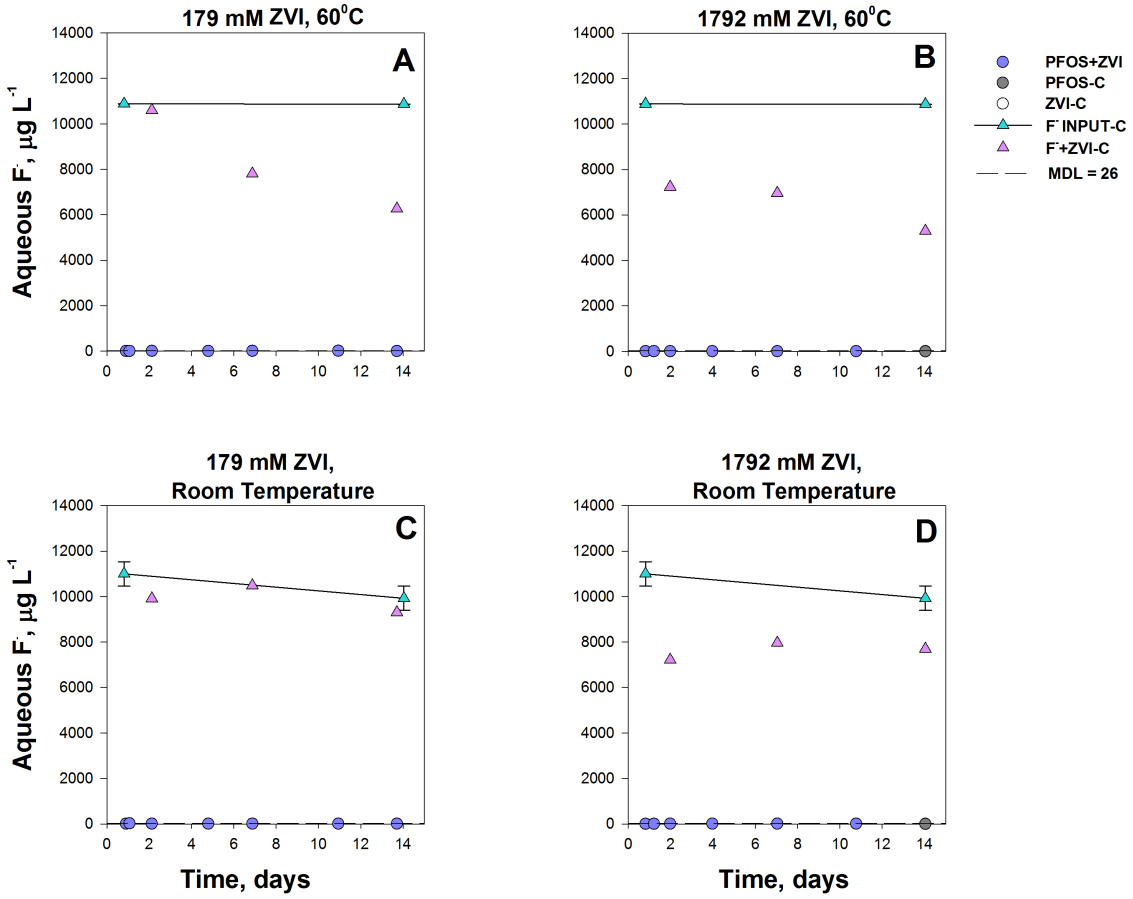

Figure 2.8 Summary of aqueous fluoride concentrations under pH_i 2.0 conditions. Figure 2.8A) 179 mM ZVI and 60°C, B) 1792 mM ZVI and 60°C, C) 179 mM ZVI and room temperature, D) 1792 mM ZVI and room temperature.

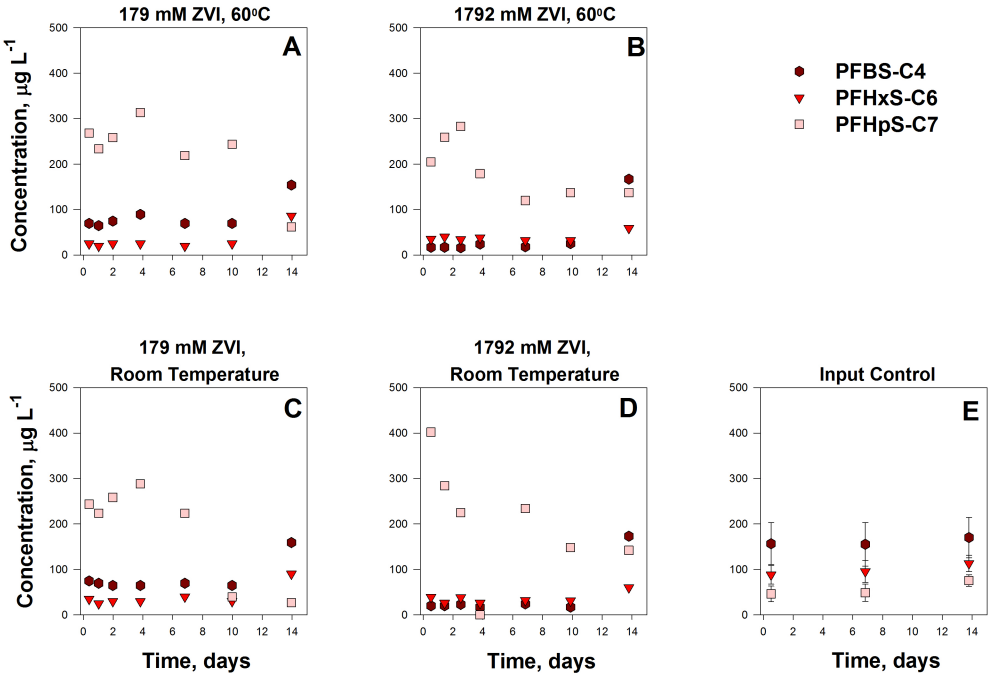

Figure 2.9 Summary of analyzed PFSA short chains present in aqueous phase under pH_i 6.6 conditions. Figure 2.9A) 179 mM ZVI and 60°C, B) 1792 mM ZVI and 60°C, C) 179 mM ZVI and room temperature, D) 1792 mM ZVI and room temperature, E) PFOS only control.

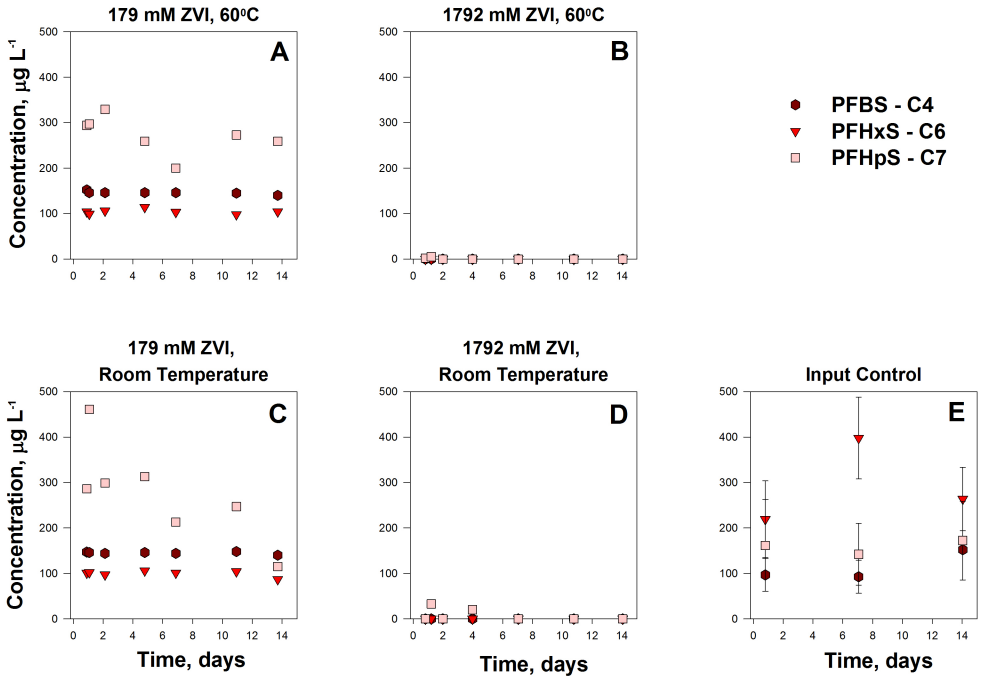

Figure 2.10 Summary of analyzed PFSA short chains present in aqueous phase under pH_i 2.0 conditions. Figure 2.10A) 179 mM ZVI and 60°C, B) 1792 mM ZVI and 60°C, C) 179 mM ZVI and room temperature, D) 1792 mM ZVI and room temperature, E) PFOS only control.

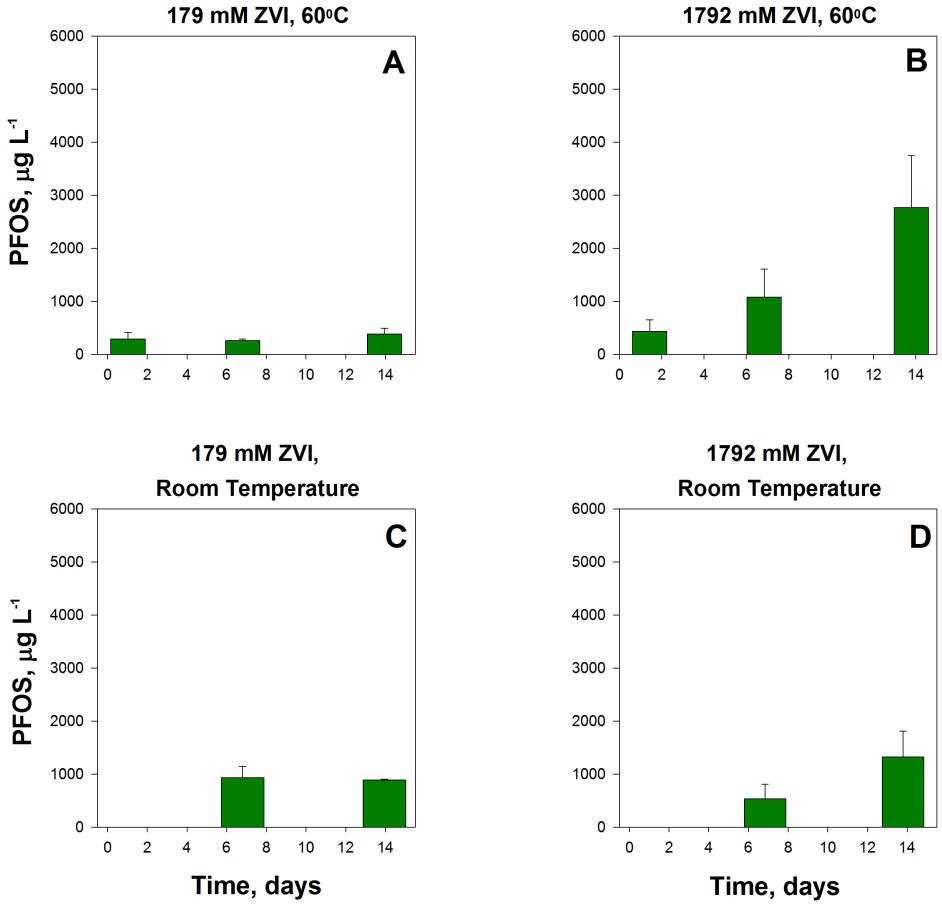

Figure 2.11 Summary of extracted PFOS from ZVI grains under pH_i 6.6 conditions. Figure 2.11A) 179 mM ZVI and 60°C, B) 1792 mM ZVI and 60°C, C) 179 mM ZVI and room temperature, D) 1792 mM ZVI and room temperature. Error bars represent error from duplicate extractions.

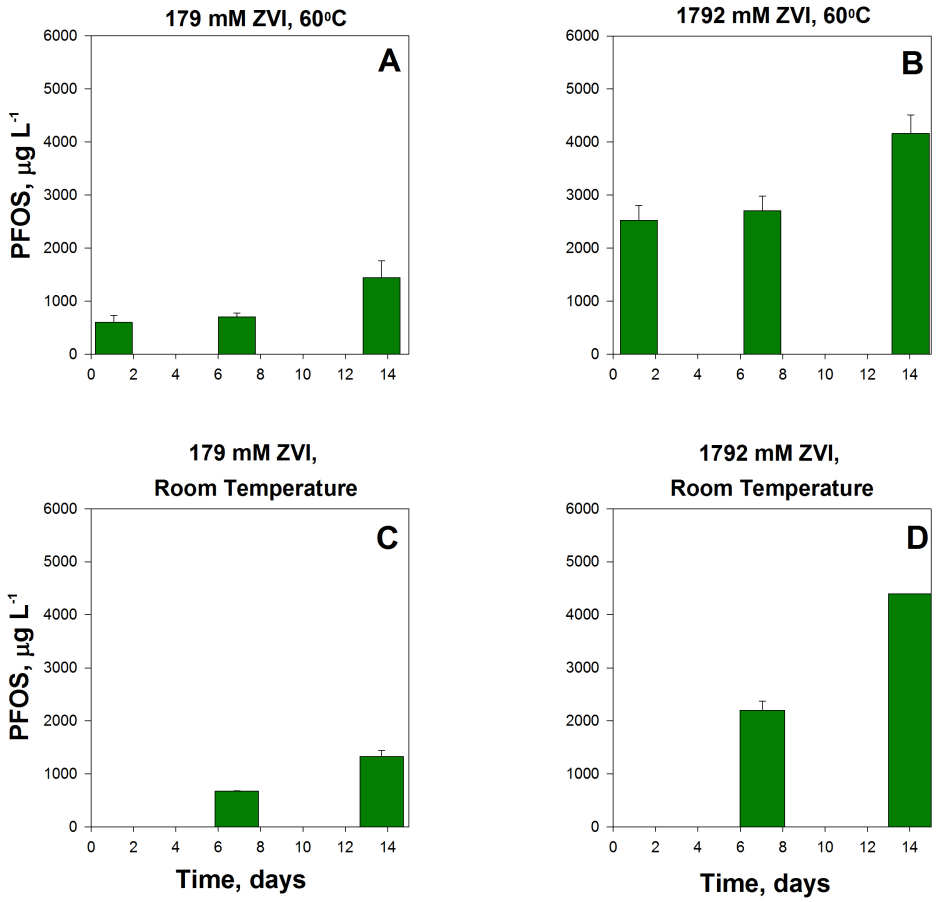

Figure 2.12 Summary of extracted PFOS from ZVI grains under pH_i 2.0 conditions. Figure 2.12A) 179 mM ZVI and 60°C, B) 1792 mM ZVI and 60°C, C) 179 mM ZVI and room temperature, D) 1792 mM ZVI and room temperature. Error bars represent error from duplicate extractions.

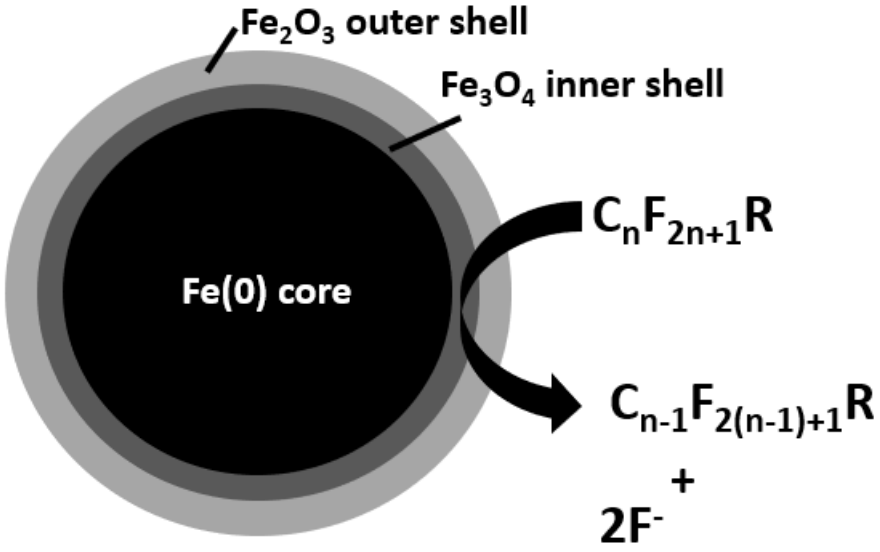

Figure 2.13 Conceptual model of PFAS removal in the presence of zerovalent iron in water, where R represents the functional group.

Table 2.1 HPLC gradient conditions used for separation of PFASs for quantification. Mobile phase is 2 mM ammonium acetate in water (Phase A) and methanol (Phase B).

Time [min]	**A [%]**	**B [%]**
0	90	10
5.0	30	70
12.0	30	70
12.1	90	10
13.0	90	10

Table 2.2 Summary of mass spectrometry conditions constant for all PFASs.

Parameter	**Value**
Gas Temperature [°C]	350
Gas Flow [L min^{-1}]	4
Nebulizer [psi]	60
Sheath Gas Temperature [°C]	350
Sheath Gas Flow [L min^{-1}]	12
Capillary [V]	3750
Nozzle Voltage [V]	0
Delta EMV, Negative Mode [V]	0

Table 2.3 Summary of the mass spectrometry ionization parameters set for each compound analyzed in the quantitative method.

Compound Name	**Precursor Ion [m/z]**	**Product Ion [m/z]**	**Fragmentor [V]**	**Collision Energy [eV]**
[^{13}C]-PFOS	503.1	98.9	180	40
[^{13}C]-PFOS	503.1	79.9	180	65
PFOS	498.9	98.9	210	50
PFOS	498.9	79.9	210	50
PFHpS	448.9	98.9	155	42
PFHpS	448.9	79.9	155	50
[^{18}O]-PFHxS	402.9	102.9	159	40
[^{18}O]-PFHxS	402.9	83.9	159	40
PFHxS	398.9	98.9	159	38
PFHxS	398.9	79.9	159	50
PFBS	298.9	98.9	80	28
PFBS	298.9	80.0	80	32

Table 2.4 Ion chromatography gradient conditions required for sufficient separation of anions needed for quantification. Mobile phase is potassium hydroxide (KOH) in ultrapure water.

Time [min]	**KOH [mM]**
0	0.5
10	0.5
30	2.0
40	8.0
45	15
60	50
63	50
63.01	0.5
65	0.5

Table 2.5 Iron analysis from dilute acid (0.5 M HCl) and circum-neutral pH (ascorbate buffer) extraction from surface of ZVI grains. ZVI grains analyzed were from batch experiments under 60°C, 1792 mM ZVI and pH_i 2.0 conditions.

Fe [mg g^{-1}]	**0.5 M HCl Extraction**		**Ascorbate Buffer Extraction**	
Time [days]	**Fe(II)**	**Fe(III)**	**Fe(II)**	**Fe(III)**
0.5	14.2	6.0	4.3	12.7
4.0	32.7	25.0	0.7	13.2
10.0	26.4	21.1	2.6	21.6

Chapter 3

Influence of Palladium Coating and pH Condition on the Removal of PFOS and PFOA in the Presence of Zerovalent Iron Nanoparticles

3.1 Executive Summary

Perfluorooctane sulfonic acid (PFOS) and perfluorooctanoic acid (PFOA) are persistent organic pollutants harmful to human and wildlife health and are resistant to degradation in the environment. PFOS and PFOA removal over a 168-hour period, when reacted with zerovalent iron nanoparticles (nZVI) under anaerobic conditions, was measured as a function of pH (pH 2.0 and pH 8.3) and nZVI surface coating (uncoated and palladium). PFOS removal from the aqueous phase after 8 hours in the presence of palladium-coated nZVI (PdnZVI) and nZVI was $\geq$ 97% under both pH conditions. However, at 168 hours the aqueous concentrations increased, representing a decline in the removal of PFOS in the presence of PdnZVI by 1 to 14%, and by 14 to 28% from the 8-hour time point in the presence of nZVI. PFOA removal from the aqueous phase after 8 hours in the presence of PdnZVI and nZVI ranged from 44 to 79% under both pH conditions. The increase of aqueous concentrations of PFOA at 168 hours compared to 8 hours was less than 4% in the presence of PdnZVI but 32 to 34% in the presence of nZVI. The decrease in PFOS and PFOA removal at later time points is attributed to changes in surface properties, as PdnZVI treated samples had a relatively smaller degree of PFOS and PFOA release compared to nZVI. Enhanced removal of PFOS and PFOA under low pH conditions at the early time suggest H^+ and its interaction with nZVI and PdnZVI may play an important role. Greater release of PFOS under low pH conditions compared to PFOA at the later time suggests the interaction of the PFASs with PdnZVI and nZVI may differ over time, depending on functional head group properties.

3.2 Introduction

Per- and polyfluoroalkyl substances (PFASs) are a class of organic surfactants which consist of linear chains of hydrocarbons where at least one hydrogen is substituted with fluorine (Fujii et al., 2007). These chains are attached to either a carboxylate or sulfonate functional group and when combined the compounds have both hydrophilic and hydrophobic properties making them ideal surfactants (Buck et al., 2011). PFASs have been manufactured since the 1940s and are used in a wide variety of applications including textile manufacturing, metal plating and aqueous film-forming foams (AFFFs) (Stock et al., 2009). The very properties that make PFASs useful also contribute to their extreme recalcitrance against natural degradation processes in the environment (Houde et al., 2006; Stock et al., 2009). Perfluorooctanoic acid (PFOA) and perfluorooctane sulfonic acid (PFOS) are the two most commonly detected PFASs in the environment. Concentrations of PFASs in groundwater near 3M Cottage Grove, a PFAS manufacturing site in MN, USA were measured as high as 846 μg L^{-1} of PFOA and 371 μg L^{-1} of PFOS (US EPA, 2009). The presence of PFASs in the environment is of serious concern primarily due to their toxicity. Mammals have been found to readily absorb PFOA and PFOS from oral and inhalation routes, where it binds to blood serum proteins and accumulates in the liver and kidneys (Plumlee et al., 2008). PFOA and PFOS have half-lives of approximately 3.8 and 5.4 years in humans, respectively (Olsen et al., 2007). Both compounds are potential carcinogens and immunotoxicants (Grandjean & Clapp, 2015).

Studies conducted at processes in wastewater treatment plants (WWTP) found that PFASs may actually increase in concentration in the effluent compared to influent (Arvaniti et al., 2012). Reverse osmosis systems are effective for PFAS removal, but may be expensive (Tang et al., 2006). Many alternative treatment materials for PFAS sorption have been studied, as the materials can be implemented in WWTPs

or for *ex situ* remediation. Studies have examined PFAS sorption onto zeolite, anaerobic sludge, biochar, alumina, silica, oil and black carbon but none are as effective as activated carbon (Chen et al., 2009; Hansen et al., 2010; Hellsing et al., 2016; Kupryianchyk et al., 2015; Ochoa-Herrera & Sierra-Alvarez, 2008; Yu et al., 2009). Sorption materials primarily transfer PFASs onto an alternative surface while ideally the contaminants of interest are degraded. Advanced oxidation processes are ineffective against PFASs, as hydroxyl radicals primarily act through hydrogen abstraction, which are not present on PFASs (Schröder & Meesters, 2005). Oxidative treatments including H_2O_2 propagation reactions, H_2O_2 with humic acids and sonochemical periodate demonstrate some PFOA removal, but its effectiveness against PFOS is unknown (Lee et al., 2016; Mitchell et al., 2014; Santos et al., 2015). Persulfate acts through sulfate radical using electron transfer and is effective for PFOA degradation when activated by heat, ultraviolet light, transition metals or in the presence of activated carbon under low pH conditions, but is fairly ineffective for PFOS degradation (Lee et al., 2012; Liu et al., 2012a; Park et al., 2016; Sun et al., 2016; Yang et al., 2013; Yin et al., 2016). PFOS appears to be removed more effectively with reductive methods than oxidative, as it is found to degrade in the presence of hydrated electrons in an anoxic alkaline solution under vacuum light and in subcritical water in the presence of zerovalent iron (ZVI) (Hori et al., 2006; Jin & Zhang, 2015). Zerovalent iron is of particular interest, as it is commonly applied in the subsurface for remediation of chlorinated organics (Mueller et al., 2012). Many studies take advantage of zerovalent iron nanoparticles (nZVI) due to the high surface area to volume ratio compared to granular iron and are thus ideally more reactive with contaminants (Li et al., 2006). The nZVI core consists of ZVI surrounded by a mixed Fe(II)/Fe(III) oxide shell in the presence of water. Under ambient conditions, ZVI is reactive in water and serves as a strong electron donor, making it a useful remediation material (Li et al., 2006).

Nanoscale ZVI can be used to complement PRBs for heavily contaminated zones or used when PRBs are impractical as an alternative remediation strategy (O'Carroll et al., 2012). Nanoparticles can be injected through wells under pressure or by gravity flow to the contaminated area and can remain in suspension with groundwater flow under certain conditions. Zhou et al. (2016), suggest that uncoated nZVI are unstable in air or moisture, oxidize easily and readily aggregate due to the large surface area and high surface energy. Coatings can be used to counteract the disadvantages of uncoated nZVI. Palladium (Pd) is the most widely used metal used in conjunction with nZVI for dehalogenation and acts as a catalyst to enhance rates of reaction with nZVI and lower the activation energy of reaction (O'Carroll et al., 2012). Some studies have observed PFAS removal in the presence of iron nanoparticles, including silica and starch coated magnetite and uncoated hematite but act primarily through sorption mechanisms (Gong et al., 2016; Lu et al., 2016; Zhou et al., 2016). Under room temperature and low pH conditions, PFOS and PFOA were removed by 86% and 38%, respectively, in the presence of magnesium amino-clay coated nZVI after 1 hour of exposure (Arvaniti et al., 2015).

Few studies to date have investigated reductive materials for effective degradation of PFOS and PFOA. Even fewer would be applicable for the subsurface aside from nZVI studies which demonstrate potential removal for PFOS and PFOA. The main objective of this study was to investigate the removal of PFOS and PFOA in the presence of nZVI. The influence of initial pH conditions and the presence of a palladium coating in conjunction with nZVI on the removal of PFOS and PFOA were also investigated.

3.3 Materials and Methods

3.3.1 Chemicals and Reagents

PFOS ($C_8F_{17}SO_3H$, $\geq$ 98%) and PFOA ($C_8HF_{15}O_2$, $\geq$ 96%) were obtained from Sigma Aldrich (Mississauga, Ontario, Canada). Isotopically labeled standards [$^{13}C_4$]-PFOS (MPFOS, $C_8F_{17}SO_3Na$, $\geq$ 99%) and [^{18}O]-PFHxS (MPFHxS, $C_6F_{13}SO_3Na$, $\geq$ 94%) were purchased from Wellington Laboratories (Guelph, Ontario, Canada) and used as internal standards. Zerovalent iron nanoparticles (nZVI) were synthesized using iron chloride hexahydrate ($FeCl_3{\cdot}6H_2O$, $\geq$ 97%, ACS), ethanol ($\geq$ 97.5%, Fisher Scientific) and sodium borohydride ($NaBH_4$, $\geq$ 98%, Anachemia). Palladium acetate ($C_{12}H_{18}O_{12}Pd_3$, 45.9-48.4% Pd, Alfa Aesar) was used to prepare palladium-coated nZVI (PdnZVI). Groundwater (0.45 μm filtered) was collected from well NC-17 located at the North Campus Site at the University of Waterloo. Methanol (HPLC-MS grade, $\geq$ 99.9%) and ammonium acetate (HPLC grade) were purchased from Sigma Aldrich (Oakville, Ontario, Canada). Ultrapure water was provided by a Milli-Q system (EMD Millipore, 18.2 MΩ·cm at 25°C).

3.3.2 nZVI Synthesis

ZVI nanoparticles were synthesized according to a method described in Huang & Ehrman (2007), with some modifications. The reaction for nZVI synthesis occurs according to (Zhang & Elliott, 2006):

$$4Fe^{3+}_{(aq)} + 3BH^{-}_{4(aq)} + 9H_2O_{(l)} \rightarrow 4Fe^{0}_{(s)} + 3H_2BO^{-}_{3(aq)} + 12H^{+}_{(aq)} + 6H_{2(g)} \qquad (3.1)$$

Briefly, a 4:1 (v/v) ethanol:water mixture was prepared, using N_2-purged ultrapure water. To generate 5.0 g Fe, 24.2 g $FeCl_3{\cdot}6H_2O$ was added to the ethanol:water

solution (Kanel et al., 2005). In a separate reactor, concentrated KOH was added to ultrapure water to make the solution alkaline, then $NaBH_4$ was added to produce a 0.2 M $NaBH_4$ solution. The $NaBH_4$ solution was filled in a burette and was added dropwise to the iron solution and stirred vigorously in a fumehood. The solid particles were brought into an anaerobic glovebox (Coy Laboratories), filtered and washed with ethanol to remove any residual water. To coat nZVI with palladium, a 1% (w/w) of Pd:Fe was added to a subset of iron nanoparticles in an ethanol solution and sonicated for 30 minutes (He et al., 2007). The synthesized nanoparticles were stored in 250 mL borosilicate bottles in the ethanol solution. On the day of the experiment, nanoparticles were washed three times with Argon-purged water and re-suspended.

3.3.3 Batch Experiment Set-Up

Batch experiments were performed to investigate PFOS and PFOA removal under multiple controlled reaction conditions (Figure 3.1). Polypropylene centrifuge tube reactors (15 mL) were transferred into an anaerobic glovebox (Coy Laboratories), and a volume of mixed PFOS and PFOA in groundwater stock was added to the reactors for a concentration of 0.2 μM each. Desired nanoparticles were re-suspended in Argon-purged ultrapure water, sonicated for 30 minutes and added to the reactors for a concentration of 90 mM. The effects of pH were examined by preparing sets of reactors with uncontrolled pH (pH = 8.3 $\pm$ 0.4, labeled as pH 8.3) or pH 2.0 $\pm$ 0.3 (labeled as pH 2.0), adjusted with hydrochloric acid. Reactors were manually shaken twice per day throughout the treatment period.

To assess PFOS/PFOA presence in the water, ultrapure water blanks were included. Controls containing nZVI and PdnZVI only were used to assess any PFOS/PFOA contribution from the nZVI/PdnZVI. PFOS and PFOA in groundwater were used as input controls to quantify the initial concentration. Controls were performed with

each batch test under the same initial pH conditions.

Samples were sacrificially taken with treatment samples collected at 3, 8, 24, 48, 72 and 168 hours and controls collected at 8, 48 and 168 hours. Aqueous samples were shaken thoroughly prior to sampling and analyzed for pH, Eh, and alkalinity inside the glovebox. Samples were then centrifuged at 6000 rpm for 20 minutes and the aqueous supernatant decanted from the solid slurry into separate 15 mL polypropylene centrifuge tubes and stored at $\leq 4°C$ until analysis.

3.3.4 Analytical Methods

Aqueous samples were equilibrated to room temperature, serially diluted by a factor of 100 and spiked with an internal standard mixture which contained 20 μg L^{-1} [^{13}C]-PFOS and [^{13}C]-PFOA (Wellington Laboratories Inc., Guelph, Canada). Samples were then passed through solid-phase extraction cartridges (Oasis HLB 3 cc 60 mg, Waters Corp., Mississauga, Canada) by gravity and concentrated by a factor of 10. The cartridges were preconditioned with 2 mL methanol (HPLC grade), washed with 2 mL ultrapure water, loaded with 20 mL sample, washed with 2 mL ultrapure water, vacuum dried for 30 seconds and eluted with 2 mL methanol. The 2 mL PFAS extracts were collected in 15 mL polypropylene centrifuge tubes and stored at $\leq 4°C$.

The concentrations of PFASs in methanol extracts were determined by high-performance liquid chromatography (1290 HPLC, Agilent Technologies, Mississauga, Canada) followed by tandem mass spectrometry (6460 QQQ, Agilent Technologies, Mississauga, Canada) equipped with an electrospray interface operated in negative mode. Methanol extracts were equilibrated to room temperature prior to analysis. A 20 μL aliquot of the methanol PFAS extract was injected and separated on an Eclipse XDB C18 column (5 μm i.d., 150 mm $\times$ 4.6 mm) (Agilent, Mississauga, Canada) maintained at 55°C. A 25 μL aliquot of the methanol PFAS extract was

injected and separated on a Kinetex C18 column (2.6 μm i.d., 100 mm $\times$ 2.1 mm) (Phenomenex, Torrance, USA) maintained at 55°C for qualitative analysis. The mobile phase consisted of 2 mM ammonium acetate in water (Phase A) and in methanol (Phase B) with a flow rate of 0.6 mL min^{-1} and gradient conditions provided in Table 3.1 for both columns. Ions were acquired in multiple reaction monitoring mode with a dwell time of 250 ms and cell accelerator voltage of 4 V. QQQ conditions and monitored parent and product ions can be found in Tables 3.2 to 3.4. A fresh calibration curve was created for each analysis and each compound had linearity in the range of 0.1 to 20 μg L^{-1} ($R^2 > 0.99$). Internal standard recovery was assessed for all samples and only quantified if within 70 and 130%. The MDLs of PFOS and PFOA were 0.4 and 1.7 μg L^{-1}.

The concentrations of fluoride in the aqueous supernatant samples were determined using ion chromatography (Dionex ICS-5000^+ DCS). Aqueous samples and standards were filtered with a 0.2 μm filter (PTFE, Pall Acrodisc) the day of analysis. A 10 μL aliquot of each sample was injected onto a column (IonPac AS18 2 $\times$ 50 mm) with a KOH eluent at a 0.25 mL min^{-1} flow rate. Gradient conditions can be found in Table 3.5. Acetate was included in the analysis due to the proximity of elution to fluoride in the presence of ZVI as found by Arvaniti et al. (2015). Fluoride and acetate were calibrated with linearity in the range of 80 to 2000 and 200 to 12500 μg L^{-1}, respectively. The MDLs of fluoride and acetate were 4 and 18 μg L^{-1}, respectively.

3.4 Results and Discussion

3.4.1 Effect of nZVI Coating on PFOS and PFOA Removal

At the 8-hour sampling time, 100% of PFOS was removed under pH 2.0 in the presence of either PdnZVI or nZVI (Figure 3.2A). The pH 8.3 conditions in the presence of PdnZVI resulted in 97% PFOS removal after 8 hours and 99% removal in the presence of nZVI (Figure 3.2B). In the presence of either PdnZVI or nZVI, highly efficient PFOS removal occurred regardless of pH conditions examined, and a statistical difference in treatment effectiveness was not observed. However, at the later sampling time of 168 hr, it was found that aqueous PFOS concentrations increased relative to the 8-hour time point, resulting in a decrease in removal. Under pH 2.0 in the presence of PdnZVI, 86% was removed after 168 hours, which is a 14% increase in PFOS concentration from the 8-hour time point (Figure 3.2A). In the presence of nZVI and pH 2.0 conditions, 70% of PFOS was removed at 168 hours, which is a 28% decrease in removal from the 8-hour time point (Figure 3.2A). After 168 hours under pH 8.3, PFOS removal was 96% and decreased by 1% in the presence of PdnZVI compared to the 8-hour time point (Figure 3.2B). In the presence of nZVI however, PFOS removal was 85% at 168 hours, a 14% decrease in removal compared to the 8-hour time point (Figure 3.2B). An observed increase in PFOS recovery over time in the presence of nZVI and PdnZVI is similar to findings observed in Park et al. (2017).

PFOA removal also occurred fairly quickly, however removal was not quite as high as PFOS, likely due differences in electrostatic and hydrophobic interactions with the iron surface (Higgins & Luthy, 2006; Park et al., 2017). Within 8 hours, 79% of initial PFOA was removed under pH 2.0 in the presence of PdnZVI and 68% removed in the presence of nZVI (Figure 3.3A). Under pH 8.3 conditions in the presence of PdnZVI,

44% of initial PFOA was removed after 8 hours and 54% removed in the presence of nZVI (Figure 3.3B). Similar to PFOS, there was not a statistically significant difference in treatment effectiveness of PdnZVI compared to nZVI under either pH condition. The degree of PFOA removal, however, remained relatively stable over time in the presence of PdnZVI treatment under both pH conditions. Under pH 2.0 conditions at 168 hr, 75% of was removed PFOA, which is a 4% decrease in removal compared to the 8-hour time point (Figure 3.3A). Under pH 8.3 conditions in the presence of PdnZVI, 47% of PFOA was removed after 168 hours, which is a 3% increase compared to the 8-hour time point (Figure 3.3B). Similar to PFOS there was, however, an increase of aqueous PFOA concentrations, representing a decline in removal, in the presence of nZVI treatment compared to PdnZVI at the 168-hour time point from the 8-hour time point. Under pH 2.0 conditions in the presence of nZVI, 36% of PFOA was removed at 168 hours, which is a 32% decrease in removal from the 8-hour time point (Figure 3.3A). Under pH 8.3 conditions in the presence of nZVI, 20% of PFOA was removed at 168 hours, which is a 34% decrease in removal from the 8-hour time point (Figure 3.3B).

Fluoride concentrations reach a maximum at 168 hours, but are also very similar to the input controls (Figure 3.4), suggesting that reductive defluorination may not be the primary removal mechanism. As nZVI appeared to allow greater PFOS and PFOA release compared to PdnZVI at the later time points, it suggests that surface properties may have an influence on this occurrence. ZVI undergoes corrosion in the presence of water according to Eqn. 3.2 and is further corroded by H^+ under acidic conditions (Eqn. 3.3):

$$Fe(0) + 2H_2O \rightarrow Fe(II) + H_2 + 2OH^- \tag{3.2}$$

$$Fe(0) + 2H^+ \rightarrow Fe(II) + H_2 \tag{3.3}$$

Over time, ZVI may be converted to iron oxides including Fe_2O_3 and $Fe(OH)_3$ based on the Schikorr equations (Schikorr, 1929):

$$3Fe(II) + 2H_2O \rightarrow Fe(II) + 2Fe(III) + H_2 + 2OH^- \tag{3.4}$$

$$Fe(II) + 2OH^- \rightarrow Fe(OH)_2 \tag{3.5}$$

$$Fe(III) + 3OH^- \rightarrow Fe(OH)_3 \tag{3.6}$$

$$3Fe(OH)_2 + 2H_2O \rightarrow FeO + Fe_2O_3 + 4H_2O + H_2 \tag{3.7}$$

$$3Fe(OH)_2 \rightarrow FeO + Fe_2O_3 + 2H_2O + H_2 \tag{3.8}$$

$$3Fe(OH)_2 \rightarrow FeO \cdot Fe_2O_3 + 2H_2O + H_2 \tag{3.9}$$

$$3Fe(OH)_2 \rightarrow Fe_3O_4 + 2H_2O + H_2 \tag{3.10}$$

The presence of Fe_3O_4 occurs as an inner oxide shell while the presence of Fe_2O_3 occurs as an outer oxide shell surrounding the reduced iron core (Odziemkowski & Simpraga, 2004) (Figure 3.5). The reduced iron core represents the anode and undergoes dissolution (Qin et al., 2004):

$$Fe(0) \rightarrow Fe(II) + 2e^- \tag{3.11}$$

Iron oxides are further corroded by the following reactions in order to reach equilibrium with the anode (Qin et al., 2004):

$$Fe_2O_3 + 6H^+ + 2e^- \rightarrow 2Fe(II) + 3H_2O \tag{3.12}$$

$$Fe_3O_4 + 8H^+ + 2e^- \rightarrow 3Fe(II) + 4H_2O \tag{3.13}$$

The corrosion process results in an increasingly porous iron oxide shell surrounding the reduced iron core over time, theoretically allowing electron transfer from the reduced core to PFOS and PFOA. Electron transfer can only occur if the Fe_2O_3 layer is sufficiently removed and if PFOS and PFOA are sorbed to the Fe_3O_4 surface (Odziemkowski & Simpraga, 2004). While PFOS and PFOA sorb to iron oxides, the time required for electron transfer may be longer than the time for corrosion of the Fe_3O_4 surface (Gong et al., 2016; Wei et al., 2017; Zhao et al., 2011; Y. Zhou et al., 2016). While reductive defluorination of the C-F bond is thermodynamically favourable in the presence of reduced iron, the bond dissociation energies are high and may require extended periods of time for electron transfer to occur (Blotevogel et al., 2017). Corrosion of the iron oxide surface may be kinetically favourable and cause the release of PFOS and PFOA into aqueous solution at later time points before reductive defluorination can occur.

The relatively smaller increase of PFOS and PFOA recovery at later time points in the presence of PdnZVI compared to nZVI under both pH conditions could indicate that the Pd coating helps reduce the impacts of iron corrosion (Eqn. 3.2, 3.3). The removal of PFOS and PFOA in the presence of PdnZVI is relatively more effective than nZVI under both pH conditions throughout the treatment period but remains susceptible to some impacts of iron corrosion on PFOS and PFOA release over time.

3.4.2 Effect of pH on PFOS and PFOA Removal

The pH of pH 2.0 batch samples remained within 2.0 ± 0.2 throughout the treatment period (Figure B.1A). The pH of pH 8.3 batch samples remained within 8.3 ± 0.4 throughout the treatment period (Figure B.1B).

Greater than 97% of PFOS was removed in the presence of PdnZVI at the 8-hour time point under both pH conditions, and there was not a statistical difference in

removal (Figure 3.6A). Some PFOS release in the presence of PdnZVI did occur at 168 hours compared to the 8-hour time point, with 86% PFOS removed under pH 2.0 conditions and 96% under pH 8.3 conditions (Figure 3.6A). In the presence of nZVI, 70% of PFOS was removed under pH 2.0 conditions and 85% under pH 8.3 conditions. Greater than 99% of PFOS was removed in the presence of nZVI at the 8-hour sampling time under either pH condition and again, no statistical difference in removal was observed (Figure 3.6B). At the 168-hour sampling time release of PFOS was observed in the presence of nZVI with 70% of PFOS removed under pH 2.0 conditions and 85% under pH 8.3 conditions. At the 168-hour time point, PFOS removal was 10% and 40% greater under pH 8.3 conditions compared to pH 2.0 conditions in the presence of PdnZVI and nZVI, respectively.

In the presence of PdnZVI at the 8-hour time point, 79% of PFOA was removed under pH 2.0 conditions and 44% was removed under pH 8.3 conditions (Figure 3.7A). Unlike PFOS, there was a similar difference in removal effectiveness for PFOA at both the 8-hour and 168-hour time points in the presence of PdnZVI, with less than a 4% change under either pH 2.0 or pH 8.3 conditions (Figure 3.7A). In the presence of nZVI at the 8-hour time point, 68% of PFOA was removed under pH 2.0 conditions and 54% under pH 8.3 conditions (Figure 3.7B). In the presence of nZVI, there was the release of PFOA at the 168-hour time point, with 36% of PFOA removed under pH 2.0 conditions and 20% under pH 8.3 conditions (Figure 3.7B). At the 8-hour time point, PFOA removal was 35% and 14% greater under pH 2.0 conditions compared to pH 8.3 conditions in the presence of PdnZVI and nZVI, respectively. The greater removal of PFOA under pH 2.0 was sustained throughout the treatment period as at the 168-hour time point, PFOA removal was 28% and 16% greater under pH 2.0 conditions compared to pH 8.3 conditions in the presence of PdnZVI and nZVI, respectively.

While there was not a statistically significant difference in PFOS or PFOA removal under pH 2.0 or pH 8.3, similar to Park et al. (2017), there does appear to be a trend in effectiveness depending on treatment exposure time and PFAS. PFOA removal is 14 to 35% greater under pH 2.0 compared to pH 8.3 conditions in the presence of either PdnZVI or nZVI at the 8-hour time point and 16 to 28% at 168 hours. The pK_a of PFOA is 2.5 which indicates that there would be a relatively greater proportion of the anionic form under low pH compared to pH 8.3 (US EPA, 2002). The isoelectric point of iron is approximately pH 7.8, indicating it would have a positive surface charge under lower pH and there could be electrostatic interaction with anionic PFOA (Higgins & Luthy, 2006; Li et al., 2006; Zhang & Elliott, 2006). Under pH 8.3 conditions, the iron surface could have zero or a negative charge and thus have minimal electrostatic interaction with anionic PFOA. PFOS removal, on the other hand, is more effective under pH 8.3 conditions at the 168-hour time point in the presence of either nZVI or PdnZVI. The pK_a of PFOS is lower than PFOA at -3.27 and thus would be anionic under either pH condition (Brooke et al., 2004). There could be rapid early-stage PFOS removal under low pH with positively charged iron due to electrostatic attraction (Ololade et al., 2016). At later time points, under low pH conditions there would relatively greater corrosion of the iron surface (Eqn 3.3, 3.12, 3.13) compared to higher pH conditions. Greater dissolution of sorptive iron oxides may explain the greater degree of PFOS release under low pH conditions. The PFOS sulfonate group is also found to be influenced by electrostatic complex and hydrogen bonds while the PFOA carboxylate group is influenced by covalent iron-carboxylate complexes (Gao & Chorover, 2012; Lu et al., 2016). Throughout the treatment, PFOA is removed to a greater degree under pH 2.0 conditions compared to pH 8.3, possibly due to electrostatic with a relatively positive ZVI surface and covalent iron-carboxylate complexes. PFOS removal is greatest at the 8-hour time point likely due

to strong electrostatic interaction with the ZVI surface under either pH condition. However, at later time points, there is a greater degree of iron oxide dissolution, especially under low pH conditions, causing a greater degree of PFOS release into the aqueous phase. The sorption mechanisms of PFOS and PFOA with iron oxides are complex, as hydrophobic interactions, ion exchange, surface complexing and hydrogen bonding may all play a role and change over time depending on the conditions (Wei et al., 2017).

3.5 Conclusions

This study demonstrated that PFOS and PFOA can be removed in the presence of nZVI and PdnZVI under both pH 2.0 and pH 8.3 conditions. However, the full initial degree of removal could not be maintained for the duration of the treatment. Low fluoride concentrations suggest reductive defluorination is not the primary removal mechanism and thus sorption and other removal mechanisms may play a greater role in PFAS removal. The influence of pH on PFOS and PFOA removal is likely due to changes to the iron surface, with a larger proportion of H^+ under lower pH conditions resulting in greater corrosion of the iron surface. PdnZVI is less impacted by iron corrosion compared to nZVI, which results in relatively less release of PFOS and PFOA at later time points. Initial removal of both PFOS and PFOA is enhanced under low pH and is likely due to electrostatic interaction. At later time points, greater dissolution of iron oxides over time under low pH conditions led to the greater release of PFOS compared to PFOA suggesting differences in the interaction of iron oxides depending on the functional head group of PFASs and presence of iron oxides. While removal of both PFOS and PFOA is greater with PdnZVI compared to nZVI, there is variable effectiveness depending on pH condition, duration and PFAS targeted. Long-

term studies investigating the influence of iron oxide forms on sorption of PFOS and PFOA under variable pH conditions are needed to understand the potential for release of PFASs.

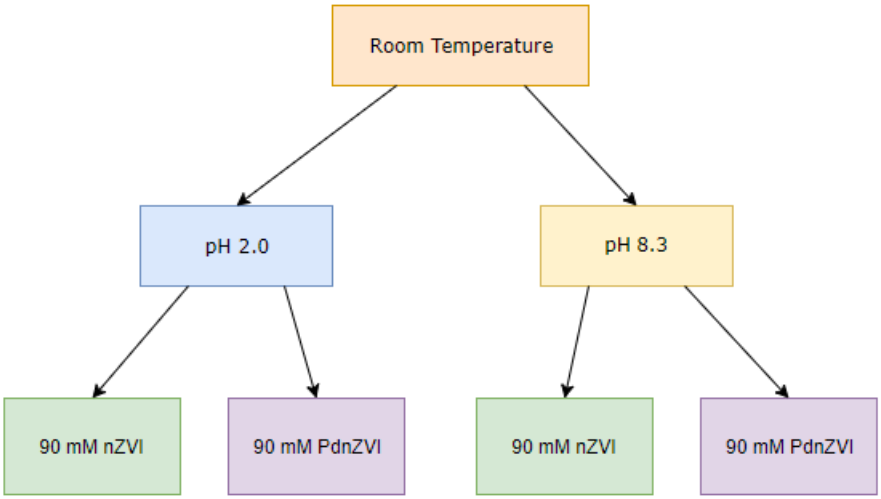

Figure 3.1 Outline of batch experiment variables for BNP. A total of 4 different conditions were examined. Room temperature is approximately 22°C. Initial pH 2.0 remained within pH 2.0 ± 0.2 (labeled as pH 2.0) throughout the treatment period for both PdnZVI and nZVI. Uncontrolled pH remained within pH 8.3 ± 0.4 (labeled as pH 8.3) for both PdnZVI and nZVI.

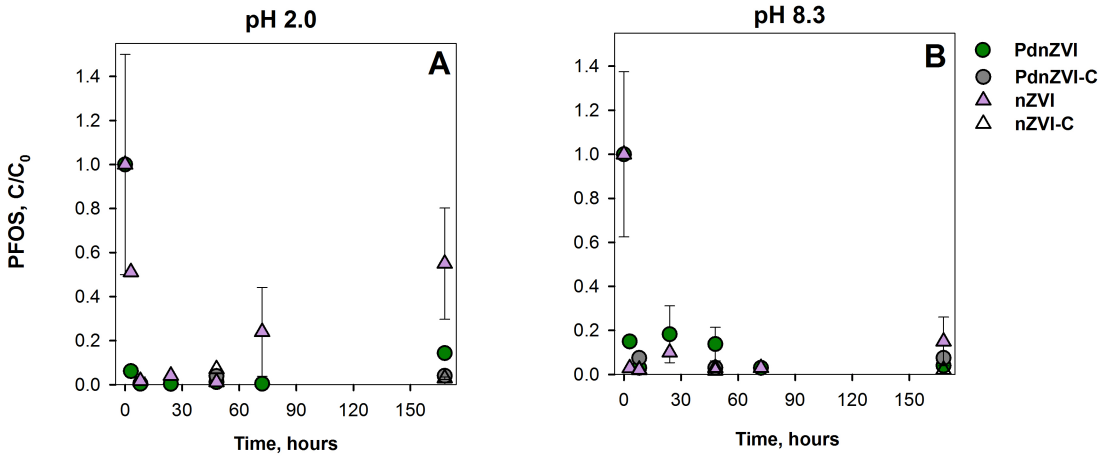

Figure 3.2 Comparison of normalized PFOS concentrations relative to initial PFOS concentration in the presence of PdnZVI or nZVI. Figure 3.2A) PFOS under pH 2.0 conditions, B) PFOS under pH 8.3 conditions. Error bars for points at 0 hours represents the standard error of the average of measured PFOS only concentration to calculate C_0. Error bars for treatment samples represent the standard error between duplicate reactors.

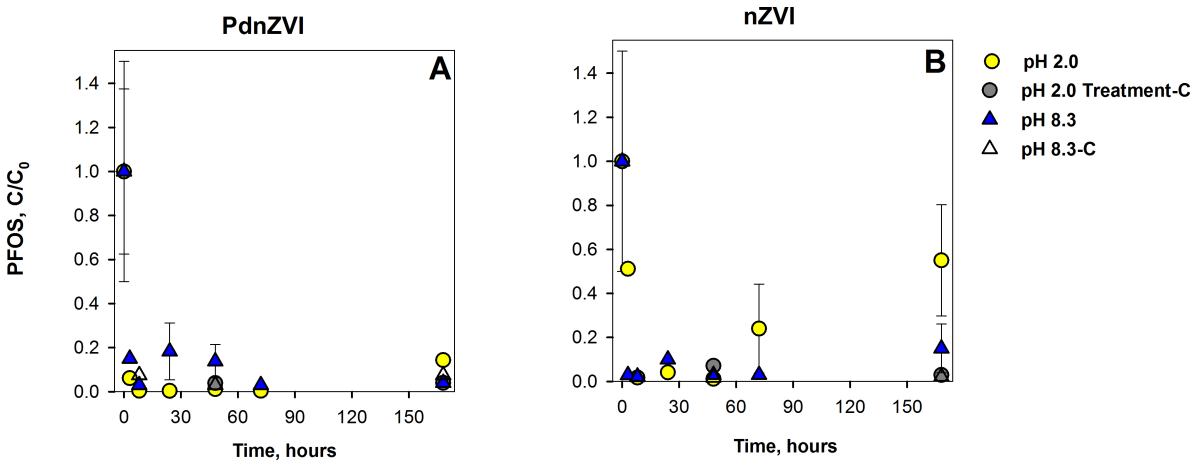

Figure 3.3 Comparison of normalized PFOA concentrations relative to initial PFOA concentration in the presence of PdnZVI or nZVI. Figure 3.3A) PFOA under pH 2.0 conditions, B) PFOA under pH 8.3 conditions. Error bars for points at 0 hours represents the standard error of the average of measured PFOA only concentration to calculate C_0. Error bars for treatment samples represent the standard error between duplicate reactors.

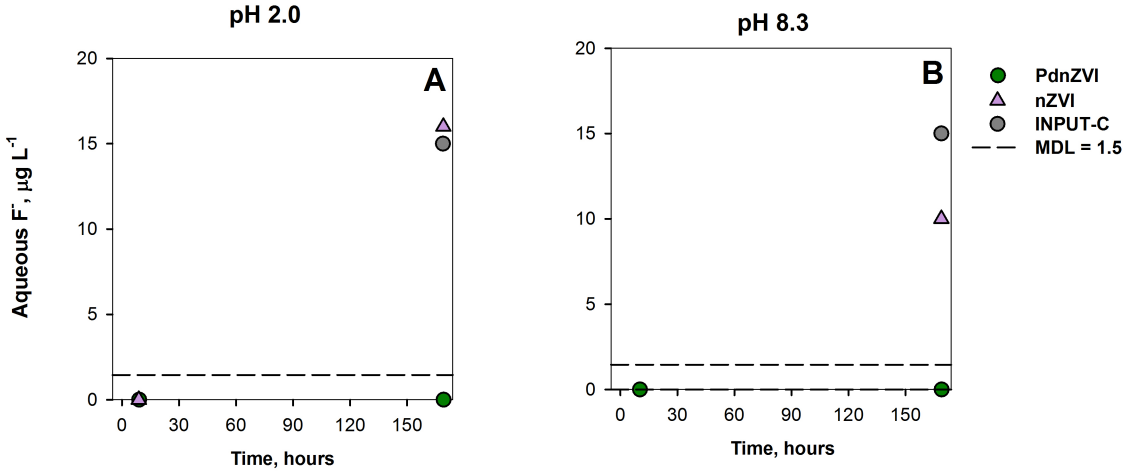

Figure 3.4 Summary of aqueous fluoride concentrations present in treatment and control samples in the presence of PdnZVI and nZVI. Figure 3.4A) pH 2.0, B) pH 8.3.

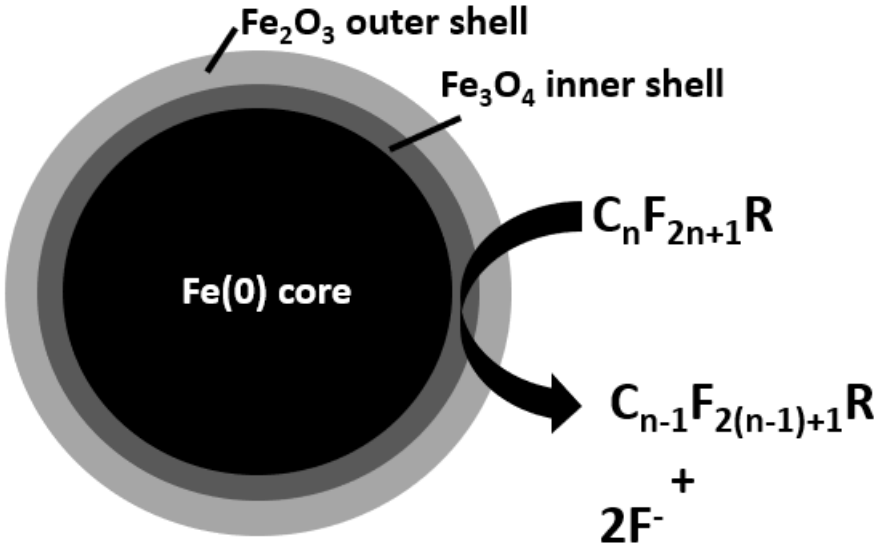

Figure 3.5 Conceptual model of PFAS removal in the presence of zerovalent iron in water, where R represents the functional group.

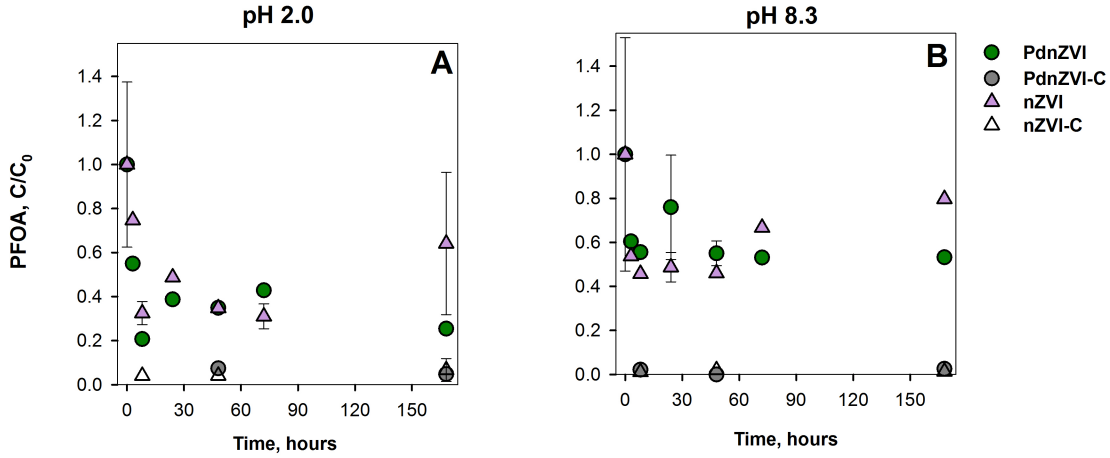

Figure 3.6 Comparison of normalized PFOS concentrations relative to initial PFOS concentration under pH 2.0 and pH 8.3 conditions. Figure 3.6A) PFOS in the presence of PdnZVI B) PFOS in the presence of nZVI. Error bars for points at 0 hours represents the standard error of the average of measured PFOS only concentration to calculate C_0. Error bars for treatment samples represent the standard error between duplicate reactors.

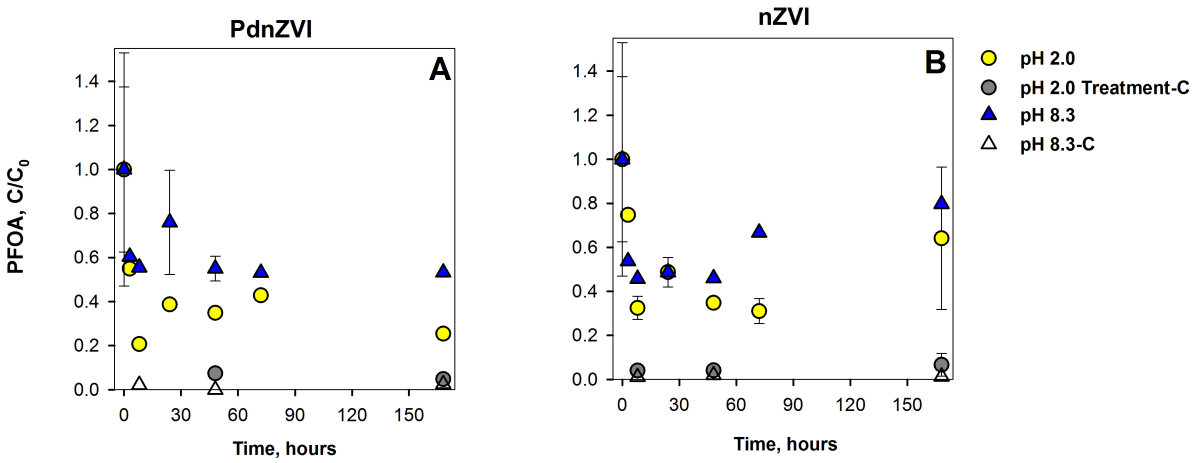

Figure 3.7 Comparison of normalized PFOA concentrations relative to initial PFOA concentration under pH 2.0 and pH 8.3 conditions. Figure 3.7A) PFOA in the presence of PdnZVI, B) PFOA in the presence of nZVI. Error bars for points at 0 hours represents the standard error of the average of measured PFOA only concentration to calculate C_0. Error bars for treatment samples represent the standard error between duplicate reactors.

Table 3.1 High-performance liquid chromatograph gradient conditions used for separation of PFASs for quantification. Mobile phase is 2 mM ammonium acetate in water (Phase A) and methanol (Phase B).

Time [min]	**A [%]**	**B [%]**
0	94	6
1	94	6
8	5	95
16	5	95
16.1	94	6
20	94	6

Table 3.2 Summary of mass spectrometry conditions constant throughout HPLC-MS/MS analysis for PFASs.

Parameter	**Value**
Gas Temperature [°C]	320
Gas Flow [L min^{-1}]	11
Nebulizer [psi]	45
Sheath Gas Temperature [°C]	350
Sheath Gas Flow [L min^{-1}]	12
Capillary [V]	3750
Nozzle Voltage [V]	0
Delta EMV, Negative Mode [V]	200

Table 3.3 Summary of the mass spectrometry ionization parameters set for each PFAS compound analyzed in the quantitative method.

Compound Name	**Precursor Ion [m/z]**	**Product Ion [m/z]**	**Fragmentor [V]**	**Collision Energy [eV]**
[^{13}C]-PFOS	503.1	99.1	170	50
[^{13}C]-PFOS	503.1	80.1	170	65
PFOS	498.9	130	210	50
PFOS	498.9	99	210	50
PFOS	498.9	80	210	50
[^{13}C]-PFOA	417.1	372	85	3
[^{13}C]-PFOA	417.1	172.1	85	12
PFOA	412.9	368.9	86	5
PFOA	412.9	219	86	5
PFOA	412.9	169	86	5

Table 3.4 Summary of the mass spectrometry ionization parameters set for each PFAS compound analyzed in the qualitative method.

Compound Name	**Precursor Ion [m/z]**	**Product Ion [m/z]**	**Fragmentor [V]**	**Collision Energy [eV]**
PFTA	712.9	669	112	9
PFTriA	662.9	619	102	9
PFDS	598.9	80	205	94
PFUA	562.9	519	92	5
PFDA	512.9	469	133	5
[^{13}C]-PFOS	503.1	99.1	170	50
[^{13}C]-PFOS	503.1	80.1	170	65
PFOS	498.9	130	210	50
PFOS	498.9	99	210	50
PFOS	498.9	80	210	50
[^{13}C]-PFOA	417.1	372	85	3
[^{13}C]-PFOA	417.1	172.1	85	12
PFOA	412.9	368.9	86	5
PFOA	412.9	219	86	5
PFOA	412.9	169	86	5
PFHxS	398.9	80	174	49
PFHpA	362.9	319	66	5
PFHxA	312.9	268.9	66	5
PFBS	298.9	80	133	45

Table 3.5 Ion chromatography gradient conditions required for sufficient separation of anions needed for quantification. Mobile phase is potassium hydroxide (KOH) in ultrapure water.

Time [min]	**KOH [mM]**
0	0.5
10	0.5
30	2.0
40	8.0
45	15
60	50
63	50
63.01	0.5
65	0.5

Chapter 4

Conclusions

Batch tests were used to investigate the impact of various conditions in conjunction with zerovalent iron (ZVI) on the removal of PFOS/PFOA from aqueous matrices. Removal effectiveness was highly variable depending on the conditions, duration and targeted compound. Low pH resulted in the higher removal of PFOS and PFOA compared to higher pH. High temperatures also improved PFOS removal over time compared to room temperature. The quantity of ZVI dosage generally improved removal, but was not always consistent and may require a greater molar ratio of ZVI:PFAS than was examined in this study. The presence of a palladium coating slightly improved PFOS and PFOA removal compared to uncoated zerovalent iron nanoparticles (nZVI) and appeared more resistant to iron corrosion over time. Fluoride concentrations and the presence of short-chain PFASs were fairly low in both studies, suggesting mineralization may not have occurred to a detectable degree. However, fluoride and ZVI only controls suggest there may be some removal of F^- from the aqueous phase due to sorption to the ZVI surface, and the amount released may have been underquantified. The lack of short-chain PFASs present in the aqueous phase may be due to the removal of intermediates or lack of production, as they were not found on the ZVI surface. Iron oxides appear to play a strong role in both studies, mainly due to greater PFOS and PFOA removal under low pH conditions which likely generates more iron oxides than under high pH conditions. Interaction of PFOS and PFOA with iron oxides is complex, as in Chapter 3 there was a greater degree of release of PFOA compared to PFOS, suggesting functional group interaction may play an important role. Greater understanding of the mechanisms involving PFAS sorption is needed as iron-PFAS complexes likely occurred but were not quantified and may help close the unknown portion of the mass balance. The application of ZVI for the remediation of PFASs in the subsurface may not be suitable for long-term removal, as the potential for release of PFASs in the presence of iron

oxides is of concern. Its general application to a suite of PFASs in groundwater may also be uncertain as treatment efficacy could vary widely depending on functional group interactions with iron surfaces.

References

Ahn, S. C., Oh, S. Y., & Cha, D. K. (2008). Enhanced reduction of nitrate by zero-valent iron at elevated temperatures. *Journal of Hazardous Materials*, *156*(1-3), 17–22. doi: 10.1016/j.jhazmat.2007.11.104

Ahrens, L. (2011). Polyfluoroalkyl compounds in the aquatic environment: a review of their occurrence and fate. *Journal of Environmental Monitoring*, *13*, 20–31. doi: 10.1039/c0em00373e

Ahrens, L., Yeung, L. W. Y., Taniyasu, S., Lam, P. K. S., & Yamashita, N. (2011). Partitioning of perfluorooctanoate (PFOA), perfluorooctane sulfonate (PFOS) and perfluorooctane sulfonamide (PFOSA) between water and sediment. *Chemosphere*, *85*(5), 731–737. doi: 10.1016/j.chemosphere.2011.06.046

Amirbahman, A., Schönenberger, R., Johnson, C. A., & Sigg, L. (1998). Aqueous- and solid-phase biogeochemistry of a calcareous aquifer system downgradient from a municipal solid waste landfill (Winterthur, Switzerland). *Environmental Science and Technology*, *32*(13), 1933–1940. doi: 10.1021/es970810j

Arvaniti, O. S., Andersen, H. R., Thomaidis, N. S., & Stasinakis, A. S. (2014). Sorption of perfluorinated compounds onto different types of sewage sludge and assessment of its importance during wastewater treatment. *Chemosphere*, *111*, 405–11. doi: 10.1016/j.chemosphere.2014.03.087

Arvaniti, O. S., Hwang, Y., Andersen, H. R., Stasinakis, A. S., Thomaidis, N. S., & Aloupi, M. (2015). Reductive degradation of perfluorinated compounds in water using Mg-aminoclay coated nanoscale zero valent iron. *Chemical Engineering Journal*, *262*, 133–139. doi: 10.1016/j.cej.2014.09.079

Arvaniti, O. S., Ventouri, E. I., Stasinakis, A. S., & Thomaidis, N. S. (2012). Occurrence of different classes of perfluorinated compounds in Greek wastewater treatment plants and determination of their solid-water distribution coefficients. *Journal of Hazardous Materials*, *239-240*, 24–31. doi: 10.1016/j.jhazmat.2012.02.015

Austin, M. E., Kasturi, B. S., Barber, M., Kannan, K., MohanKumar, P. S., & MohanKumar, S. M. (2003). Neuroendocrine effects of perfluorooctane sulfonate in rats. *Environmental Health Perspectives*, *111*(12), 1485–1489. doi: 10.1289/ehp.6128

Boparai, H., Joseph, M., & O'Carroll, D. M. (2011). Kinetics and thermodynamics of cadmium ion removed by adsorption onto zerovalent iron particles. *Journal of Hazardous Materials*, *186*, 458–465. doi: 10.1016/j.jhazmat.2010.11.029

Boudreau, T. M., Wilson, C. J., Cheong, W. J., Sibley, P. K., Mabury, S. a., Muir, D. C. G., & Solomon, K. R. (2003). Response of the zooplankton community and environmental fate of perfluorooctane sulfonic acid in aquatic microcosms. *Environmental Toxicology and Chemistry*, *22*(11), 2739–45. doi: 10.1897/02-394

Brooke, D., Footitt, A., & Nwaogu, T. A. (2004). *Environmental Risk Evaluation Report: Perfluorooctanesulphonate (PFOS).* Environment Agency.

Buck, R. C., Franklin, J., Berger, U., Conder, J. M., Cousins, I. T., Voogt, P. D., ... van Leeuwen, S. P. J. (2011). Perfluoroalkyl and polyfluoroalkyl substances in the

environment: Terminology, classification, and origins. *Integrated Environmental Assessment and Management*, *7*(4), 513–541. doi: 10.1002/ieam.258

Chen, H., Chen, S., Quan, X., Zhao, Y., & Zhao, H. (2009). Sorption of perfluorooctane sulfonate (PFOS) on oil and oil-derived black carbon: influence of solution pH and [Ca2+]. *Chemosphere*, *77*(10), 1406–1411. doi: 10.1016/j.chemosphere.2009.09.008

DWC. (2006). *Provisional evaluation of PFT in drinking water with the guide substances perfluorooctanoic acid (PFOA) and perfluorooctane sulfonate (PFOS) as examples.* Drinking Water Commission of the German Ministry of Health. Retrieved from http://www.umweltbundesamt.de/sites/default/files/medien/pdfs/pft-in-drinking-water.pdf

DWI. (2009). *Guidance on the Water Supply (Water Quality) Regulations 2000 specific to PFOS (Perfluorooctane Sulphonate) and PFOA (Perfluorooctanoic Acid) Concentrations in Drinking Water.* Drinking Water Inspectorate. London. Retrieved from http://www.dwi.gov.uk/stakeholders/information-letters/2009/10{_}2009annex.pdf

Environment Canada. (2013). *Perfluorooctane Sulfonate in the Canadian Environment.* Environment Canada.

Fang, Z., Chen, J., Qiu, X., Qiu, X., Cheng, W., & Zhu, L. (2011). Effective removal of antibiotic metronidazole from water by nanoscale zero-valent iron particles. *Desalination*, *268*(1-3), 60–67. doi: 10.1016/j.desal.2010.09.051

Fu, F., Dionysiou, D. D., & Liu, H. (2014). The use of zero-valent iron for groundwater remediation and wastewater treatment: A review. *Journal of Hazardous Materials*, *267*, 194–205. doi: 10.1016/j.jhazmat.2013.12.062

Fujii, S., Tanaka, S., Hong Lien, N. P., Qiu, Y., & Polprasert, C. (2007). New POPs in the water environment: distribution, bioaccumulation and treatment of perfluorinated compounds a review paper. *Journal of Water Supply*, *56*(5), 313–326. doi: 10.2166/aqua.2007.005

Gao, X., & Chorover, J. (2012). Adsorption of perfluorooctanoic acid and perfluorooctanesulfonic acid to iron oxide surfaces as studied by flow-through ATR-FTIR spectroscopy. *Environmental Chemistry*, *9*(2), 148–157. doi: 10.1071/EN11119

Gewurtz, S. B., Backus, S. M., De Silva, A. O., Ahrens, L., Armellin, A., Evans, M., ... Waltho, J. (2013). Perfluoroalkyl acids in the Canadian environment: multimedia assessment of current status and trends. *Environment International*, *59*, 183–200. doi: 10.1016/j.envint.2013.05.008

Gibbs, M. M. (1979). A simple method for the rapid determination of iron in natural waters. *Water Research*, *13*(3), 295–297. doi: 10.1016/0043-1354(79)90209-4

Gong, Y., Wang, L., Liu, J., Tang, J., & Zhao, D. (2016). Removal of aqueous perfluorooctanoic acid (PFOA) using starch-stabilized magnetite nanoparticles. *Science of The Total Environment*, *562*, 191–200. doi: 10.1016/j.scitotenv.2016.03.100

Grandjean, P., & Clapp, R. (2015). Perfluorinated Alkyl Substances: Emerging Insights Into Health Risks. *NEW SOLUTIONS: A Journal of Environmental and Occupational Health Policy*. doi: 10.1177/1048291115590506

Hansen, M. C., Børresen, M. H., Schlabach, M., & Cornelissen, G. (2010). Sorption of perfluorinated compounds from contaminated water to activated carbon. *Journal of Soils and Sediments*, *10*(2), 179–185. doi: 10.1007/s11368-009-0172-z

He, F., Zhao, D., Liu, J., & Roberts, C. B. (2007). Stabilization of Fe - Pd nanoparticles with sodium carboxymethyl cellulose for enhanced transport and dechlorination

of trichloroethylene in soil and groundwater. *Industrial and Engineering Chemistry Research*, *46*(1), 29–34. doi: 10.1021/ie0610896

Health Canada. (2016a). *Perfluorooctane Sulfonate (PFOS) in Drinking Water.* Health Canada.

Health Canada. (2016b). *Perfluorooctanoic Acid (PFOA) in Drinking Water.* Health Canada.

Hellsing, M. S., Josefsson, S., Hughes, A. V., & Ahrens, L. (2016). Sorption of perfluoroalkyl substances to two types of minerals. *Chemosphere*, *159*, 385–391. doi: 10.1016/j.chemosphere.2016.06.016

Heron, G., Crouzet, C., Bourg, A. C. M., & Christensen, T. H. (1994). Speciation of Fe (II) and Fe (III) in contaminated aquifer sediments using chemical extraction techniques. *Environmental Science & Technology*, *28*(9), 1698–1705. doi: 10.1021/es00058a023

Higgins, C. P., & Luthy, R. G. (2006). Sorption of perfluorinated surfactants on sediments. *Environmental Science and Technology*, *40*(23), 7251–7256. doi: 10.1021/es061000n

Hoffman, K., Webster, T., Bartell, S., Weisskopf, M., Fletcher, T., & Vieira, V. (2010). Private drinking water wells as a source of exposure to perfluorooctanoic acid (PFOA) in communities surrounding a fluoropolymer production facility. *Environmental Health Perspectives*, *119*(1), 91. doi: http://dx.doi.org/10.1289/ehp.1002503

Hori, H., Nagaoka, Y., Yamamoto, A., Sano, T., Yamashita, N., Taniyasu, S., ... Arakawa, R. (2006). Efficient decomposition of environmentally persistent perflu-

orooctanesulfonate and related fluorochemicals using zerovalent iron in subcritical water. *Environmental Science & Technology*, *40*(3), 1049–54.

Houde, M., Martin, J., Letcher, R. J., Solomon, K. R., & Muir, D. (2006). Critical Review Biological Monitoring of Polyfluoroalkyl Substances: A Review. *Environmental Science & Technology*, *40*(11), 3463–3473. doi: 10.1021/es052580b

Houtz, E. F., Higgins, C. P., Field, J. a., & Sedlak, D. L. (2013). Persistence of perfluoroalkyl acid precursors in AFFF-impacted groundwater and soil. *Environmental Science and Technology*, *47*, 8187–8195. doi: 10.1021/es4018877

Hu, Z., Song, X., Wei, C., & Liu, J. (2017). Chemosphere Behavior and mechanisms for sorptive removal of perfluorooctane sulfonate by layered double hydroxides. *Chemosphere*, *187*, 196–205.

Huang, K. C., & Ehrman, S. H. (2007). Synthesis of iron nanoparticles via chemical reduction with palladium ion seeds. *Langmuir*, *23*(3), 1419–1426. doi: 10.1021/la0618364

Jensen, A. A., & Leffers, H. (2008). Emerging endocrine disrupters: Perfluoroalkylated substances. *International Journal of Andrology*, *31*(2), 161–169. doi: 10.1111/j.1365-2605.2008.00870.x

Jin, L., & Zhang, P. (2015). Photochemical decomposition of perfluorooctane sulfonate (PFOS) in an anoxic alkaline solution by 185 nm vacuum ultraviolet. *Chemical Engineering Journal*. doi: 10.1016/j.cej.2015.06.022

Johnson, R. L., Anschutz, A. J., Smolen, J. M., Simcik, M. F., & Lee Penn, R. (2007). The adsorption of perfluorooctane sulfonate onto sand, clay, and iron oxide surfaces. *Journal of Chemical and Engineering Data*, *52*(4), 1165–1170. doi: 10.1021/je060285g

Kanel, S. R., Manning, B., Charlet, L., & Choi, H. (2005). Removal of Arsenic (III) from Groundwater by Nanoscale Zero-Valent Iron. *Environmental Science & Technology*, *39*(5), 1291–1298. doi: 10.1021/es048991u

Kannan, K. (2011). Perfluoroalkyl and polyfluoroalkyl substances: Current and future perspectives. *Environmental Chemistry*, *8*, 333–338. doi: 10.1071/EN11053

Key, B. D., Howell, R. D., & Criddle, C. S. (1998). Defluorination of Organofluorine Sulfur Compounds by Pseudomonas Sp. Strain D2. *Environmental Science and Technology*, *32*(15), 2283–2287. doi: S0013-936X(98)00012-1

Khan, A., Prabhu, S. M., Park, J., Lee, W., Chon, C. M., Ahn, J. S., & Lee, G. (2017). Azo dye decolorization by ZVI under circum-neutral pH conditions and the characterization of ZVI corrosion products. *Journal of Industrial and Engineering Chemistry*, *47*, 86–93. doi: 10.1016/j.jiec.2016.11.017

Kissa, E. (1994). *Fluorinated surfactants: Synthesis, properties, applications*. Dekker.

Kupryianchyk, D., Hale, S. E., Breedveld, G. D., & Cornelissen, G. (2015). Treatment of sites contaminated with perfluorinated compounds using biochar amendment. *Chemosphere*, *142*, 35–40. doi: 10.1016/j.chemosphere.2015.04.085

Lau, C., Anitole, K., Hodes, C., Lai, D., Pfahles-Hutchens, A., & Seed, J. (2007). Perfluoroalkyl acids: A review of monitoring and toxicological findings. *Toxicological Sciences*, *99*(2), 366–394. doi: 10.1093/toxsci/kfm128

Lau, C., Thibodeaux, J. R., Hanson, R. G., Narotsky, M. G., Rogers, J. M., Lindstrom, A. B., & Strynar, M. J. (2006). Effects of perfluorooctanoic acid exposure during pregnancy in the mouse. *Toxicological Sciences*, *90*(2), 510–518. doi: 10.1093/toxsci/kfj105

Lee, Y. C., Chen, M. J., Huang, C. P., Kuo, J., & Lo, S. L. (2016). Efficient sonochemical degradation of perfluorooctanoic acid using periodate. *Ultrasonics Sonochemistry*, *31*, 499–505. doi: 10.1016/j.ultsonch.2016.01.030

Lee, Y. C., Lo, S. L., Chiueh, P. T., & Chang, D. G. (2009). Efficient decomposition of perfluorocarboxylic acids in aqueous solution using microwave-induced persulfate. *Water Research*, *43*(11), 2811–2816. doi: 10.1016/j.watres.2009.03.052

Lee, Y. C., Lo, S. L., Chiueh, P. T., Liou, Y. H., & Chen, M. L. (2010). Microwave-hydrothermal decomposition of perfluorooctanoic acid in water by iron-activated persulfate oxidation. *Water Research*, *44*(3), 886–92. doi: 10.1016/j.watres.2009.09.055

Lee, Y. C., Lo, S. L., Kuo, J., & Lin, Y. L. (2012). Persulfate oxidation of perfluorooctanoic acid under the temperatures of 20-40°C. *Chemical Engineering Journal*, *198-199*, 27–32. doi: 10.1016/j.cej.2012.05.073

Li, X.-q., Elliott, D. W., & Zhang, W.-x. (2006). Zero-Valent Iron Nanoparticles for Abatement of Environmental Pollutants: Materials and Engineering Aspects. *Critical Reviews in Solid State and Materials Sciences*, *31*(4), 111–122. doi: 10.1080/10408430601057611

Liu, C. S., Higgins, C. P., Wang, F., & Shih, K. (2012a). Effect of temperature on oxidative transformation of perfluorooctanoic acid (PFOA) by persulfate activation in water. *Separation and Purification Technology*, *91*, 46–51. doi: 10.1016/j.seppur.2011.09.047

Liu, C. S., Shih, K., & Wang, F. (2012b). Oxidative decomposition of perfluorooctanesulfonate in water by permanganate. *Separation and Purification Technology*, *87*, 95–100. doi: 10.1016/j.seppur.2011.11.027

Liu, S., Lu, Y., Xie, S., Wang, T., Jones, K. C., & Sweetman, A. J. (2015). Exploring the fate, transport and risk of Perfluorooctane Sulfonate (PFOS) in a coastal region of China using a multimedia model. *Environment International*, *85*, 15–26. doi: 10.1016/j.envint.2015.08.007

Lu, X., Deng, S., Wang, B., Huang, J., Wang, Y., & Yu, G. (2016). Adsorption behavior and mechanism of perfluorooctane sulfonate on nanosized inorganic oxides. *Journal of Colloid and Interface Science*, *474*, 199–205. doi: 10.1016/j.jcis.2016.04.032

Manning, B. A., Hunt, M. L., Amrhein, C., & Yarmoff, J. A. (2002). Arsenic(III) and arsenic(V) reactions with zerovalent iron corrosion products. *Environmental Science and Technology*, *36*(24), 5455–5461. doi: 10.1021/es0206846

Merino, N., Qu, Y., Deeb, R. A., Hawley, E. L., Hoffmann, M. R., & Mahendra, S. (2016). Degradation and Removal Methods for Perfluoroalkyl and Polyfluoroalkyl Substances in Water. *Environmental Engineering Science*, *33*(9), 615–649. doi: 10.1089/ees.2016.0233

Mitchell, S. M., Ahmad, M., Teel, A. L., & Watts, R. J. (2014). Degradation of Perfluorooctanoic Acid by Reactive Species Generated through Catalyzed H2O2 Propagation Reactions. *Environmental Science & Technology Letters*, *1*(1), 117–121. doi: 10.1021/ez4000862

Moermond, C., Verbruggen, E., & Smit, C. (2010). *Environmental risk limits for PFOS.* National Institute for Public Health and the Environment.

Moody, C., & Field, J. (1999). Determination of Perfluorocarboxylates in Groundwater Impacted by Fire-Fighting Activity. *Environmental Science and Technology*, *33*(16), 2800–2806. doi: 10.1021/es981355+

Moody, C. A., Hebert, G. N., Strauss, H., & Field, J. A. (2003). Occurrence and persistence of perfluorooctanesulfonate and other perfluorinated surfactants in groundwater at a fire-training area at Wurtsmith Air Force Base, Michigan, USA. *Journal of Environmental Monitoring*, *5*, 341–345. doi: 10.1039/b212497a

Mueller, N. C., Braun, J., Bruns, J., Černík, M., Rissing, P., Rickerby, D., & Nowack, B. (2012). Application of nanoscale zero valent iron (NZVI) for groundwater remediation in Europe. *Environmental Science and Pollution Research*, *19*(2), 550–558. doi: 10.1007/s11356-011-0576-3

O'Carroll, D., Sleep, B., Krol, M., Boparai, H., & Kocur, C. (2012). Nanoscale zero valent iron and bimetallic particles for contaminated site remediation. *Advances in Water Resources*, *51*, 104–122. doi: 10.1016/j.advwatres.2012.02.005

Ochoa-Herrera, V., & Sierra-Alvarez, R. (2008). Removal of perfluorinated surfactants by sorption onto granular activated carbon, zeolite and sludge. *Chemosphere*, *72*(10), 1588–1593. doi: 10.1016/j.chemosphere.2008.04.029

Ochoa-Herrera, V., Sierra-Alvarez, R., Somogyi, A., Jacobsen, N. E., Wysocki, V. H., & Field, J. a. (2008). Reductive defluorination of perfluorooctane sulfonate. *Environmental Science and Technology*, *42*(9), 3260–3264. doi: 10.1021/es702842q

Odziemkowski, M. S., & Simpraga, R. P. (2004). Distribution of oxides on iron materials used for remediation of organic groundwater contaminants Implications for hydrogen evolution reactions. *Canadian Journal of Chemistry*, *82*(10), 1495–1506. doi: 10.1139/v04-120

Ololade, I. A., Zhou, Q., & Pan, G. (2016). Influence of oxic/anoxic condition on sorption behavior of PFOS in sediment. *Chemosphere*, *150*, 798–803. doi: 10.1016/j.chemosphere.2015.08.068

Olsen, G. W., Burris, J. M., Ehresman, D. J., Froelich, J. W., Seacat, A. M., Butenhoff, J. L., & Zobel, L. R. (2007). Half-life of serum elimination of perfluorooctanesulfonate, perfluorohexanesulfonate, and perfluorooctanoate in retired fluorochemical production workers. *Environmental Health Perspectives*, *115*(9), 1298–1305. doi: 10.1289/ehp.10009

Park, S., Lee, L. S., Medina, V. F., Zull, A., & Waisner, S. (2016). Heat-activated persulfate oxidation of PFOA, 6:2 fluorotelomer sulfonate, and PFOS under 4 conditions suitable for in-situ remediation of groundwater. *Chemosphere*, *145*, 376–383. doi: 10.1016/j.chemosphere.2015.11.097

Park, S., Zenobio, J. E., & Lee, L. S. (2017). Perfluorooctane sulfonate (PFOS) removal with Pd0/nFe0 nanoparticles: Adsorption or aqueous Fe-complexation, not transformation? *Journal of Hazardous Materials*, *342*, 20–28. doi: 10.1016/j.jhazmat.2017.08.001

Pedersen, H. D., Postma, D., Jakobsen, R., & Larsen, O. (2005). Fast transformation of iron oxyhydroxides by the catalytic action of aqueous Fe(II). *Geochimica et Cosmochimica Acta*, *69*(16), 3967–3977. doi: 10.1016/j.gca.2005.03.016

Plumlee, M. H., Larabee, J., & Reinhard, M. (2008). Perfluorochemicals in water reuse. *Chemosphere*, *72*(10), 1541–1547. doi: 10.1016/j.chemosphere.2008.04.057

Prasad, P. V., Das, C., & Golder, A. K. (2011). Reduction of Cr(VI) to Cr(III) and removal of total chromium from wastewater using scrap iron in the form of zerovalent iron(ZVI): Batch and column studies. *Canadian Journal of Chemical Engineering*, *89*(6), 1575–1582. doi: 10.1002/cjce.20590

Prevedouros, K., Cousins, I., Buck, R., & Korzeniowski, S. (2006). Sources, Fate and Transport of Perfluorocarboxylates. *Environmental Science & Technology*, *40*(1), 32–44. doi: 10.1021/es0512475

Qin, Z., Demko, B., Noël, J., Shoesmith, D., King, F., Worthingham, R., & Keith, K. (2004). Localized dissolution of millscale-covered pipeline steel surfaces. *Corrosion*, *60*(10), 906–914. doi: 10.5006/1.3287824

Qu, Y., Zhang, C.-J., Chen, P., Zhou, Q., & Zhang, W.-X. (2014). Effect of initial solution pH on photo-induced reductive decomposition of perfluorooctanoic acid. *Chemosphere*, *107*, 218–223. doi: 10.1016/j.chemosphere.2013.12.046

Rayne, S., & Forest, K. (2009). Perfluoroalkyl sulfonic and carboxylic acids: a critical review of physicochemical properties, levels and patterns in waters and wastewaters, and treatment methods. *Journal of Environmental Science and Health, Part A*, *44*(12), 1145–1199. doi: 10.1080/10934520903139811

Sáez, M., de Voogt, P., & Parsons, J. R. (2008). Persistence of perfluoroalkylated substances in closed bottle tests with municipal sewage sludge. *Environmental Science and Pollution Research*, *15*(6), 472–477. doi: 10.1007/s11356-008-0020-5

Saha, A., & Sinha, A. (2015). Current trend on application of Zero-Valent Iron (ZVI) for dehalogenation of Organo Chlorine Pesticides. *Discovery*, *40*(183), 167–174.

Sanderson, H., Boudreau, T. M., Mabury, S. A., & Solomon, K. R. (2004). Effects of perfluorooctane sulfonate and perfluorooctanoic acid on the zooplanktonic community. *Ecotoxicology and Environmental Safety*, *58*(1), 68–76. doi: 10.1016/j.ecoenv.2003.09.012

Santos, A., Rodríguez, S., Pardo, F., & Romero, A. (2015). Use of Fenton reagent combined with humic acids for the removal of PFOA from contaminated water. *Science of the Total Environment*.

Schikorr, G. (1929). Über die reaktionen zwischen eisen, seinen hydroxyden und wasser. *Berichte der Bunsengesellschaft für physikalische Chemie*, *35*(2), 65–70. doi: 10.1002/bbpc.19290350204

Schröder, H. F., & Meesters, R. J. W. (2005). Stability of fluorinated surfactants in advanced oxidation processes - A follow up of degradation products using flow injection-mass spectrometry, liquid chromatography-mass spectrometry and liquid chromatography-multiple stage mass spectrometry. *Journal of Chromatography A*, *1082*(1), 110–119. doi: 10.1016/j.chroma.2005.02.070

Schwertmann, U., & Murad, E. (1983). Effect of pH on the Formation of Goethite and Hematite from Ferrihydrite. *Clays and Clay Minerals*, *31*(4), 277–284. doi: 10.1346/CCMN.1983.0310405

Skutlarek, D., Exner, M., & Färber, H. (2006). Perfluorinated surfactants in surface and drinking waters. *Environmental Science and Pollution Research*, *13*(5), 299–307. doi: http://dx.doi.org/10.1065/espr2006.07.326

Stock, N., Muir, D., & Mabury, S. (2009). Persistent organic pollutants. In S. Harrad (Ed.), (pp. 25–69). UK: John Wiley & Sons.

Sujana, M. G., Soma, G., Vasumathi, N., & Anand, S. (2009). Studies on fluoride adsorption capacities of amorphous Fe/Al mixed hydroxides from aqueous solutions. *Journal of Fluorine Chemistry*, *130*(8), 749–754. doi: 10.1016/j.jfluchem.2009.06.005

Sun, B., Ma, J., & Sedlak, D. L. (2016). Chemisorption of perfluorooctanoic acid on powdered activated carbon initiated by persulfate in aqueous solution. *Environmental Science & Technology*. doi: 10.1021/acs.est.6b00411

Tang, C., Fu, S., Robertson, A., Criddle, C., & Leckie, J. (2006). Use of Reverse Osmosis Membranes to Remove Perfluorooctane Sulfonate (PFOS) from Semiconductor Wastewater. *Environmental Science & Technology*, *40*(23), 7343–7349. doi: 10.1021/es060831q

Tsitonaki, A., Petri, B., Crimi, M., Mosbæk, H., Siegrist, R. L., & Bjerg, P. L. (2010). In Situ Chemical Oxidation of Contaminated Soil and Groundwater Using Persulfate: A Review. *Critical Reviews in Environmental Science and Technology*, *40*, 55–91. doi: 10.1080/10643380802039303

US EPA. (2002). *Hazard assessment of perfluorooctanoic acid and its salts.* US Environmental Protection Agency.

US EPA. (2009). *Long-Chain Perfluorinated Chemicals (PFCs) Action Plan.* US Environmental Protection Agency.

US EPA. (2014). *Emerging Contaminants Perfluorooctane Sulfonate (PFOS) and Perfluorooctanoic Acid (PFOA).* US Environmental Protection Agency.

US EPA. (2016). *PFOA &PFOS Drinking Water Health Advisories.* US Environmental Protection Agency.

Vecitis, C. D., Park, H., Cheng, J., Mader, B. T., & Hoffmann, M. R. (2009). Treatment technologies for aqueous perfluorooctanesulfonate (PFOS) and perfluorooctanoate (PFOA). *Frontiers of Environmental Science and Engineering in China*, *3*(2), 129–151. doi: 10.1007/s11783-009-0022-7

Vellanki, B. P., Abdel-wahab, A., & Batchelor, B. (2013). Advanced Reduction Processes: A New Class of Treatment Processes. *Environmental Engineering Science*, *30*(5), 264–271. doi: 10.1089/ees.2012.0273

Voogt, P., & Saez, M. (2006). Analytical chemistry of perfluoroalkylated substances. *Trends in Analytical Chemistry*, *25*(4), 326–342. doi: 10.1016/j.trac.2005.10.008

Wei, C., Song, X., Wang, Q., & Hu, Z. (2017). Sorption kinetics, isotherms and mechanisms of PFOS on soils with different physicochemical properties. *Ecotoxicology and Environmental Safety*, *142*, 40–50. doi: 10.1016/j.ecoenv.2017.03.040

Xie, S., Lu, Y., Wang, T., Liu, S., Jones, K., & Sweetman, A. (2013). Estimation of PFOS emission from domestic sources in the eastern coastal region of China. *Environment International*, *59*, 336–343. doi: 10.1016/j.envint.2013.06.015

Yang, S., Cheng, J., Sun, J., Hu, Y., & Liang, X. (2013). Defluorination of aqueous perfluorooctanesulfonate by activated persulfate oxidation. *PloS ONE*, *8*(10), e74877. doi: 10.1371/journal.pone.0074877

Yin, P., Hu, Z., Song, X., Liu, J., & Lin, N. (2016). Activated Persulfate Oxidation of Perfluorooctanoic Acid (PFOA) in Groundwater under Acidic Conditions. *International Journal of Environmental Research and Public Health*, *13*(602). doi: 10.3390/ijerph13060602

Yu, J., Hu, J., Tanaka, S., & Fujii, S. (2009). Perfluorooctane sulfonate (PFOS) and perfluorooctanoic acid (PFOA) in sewage treatment plants. *Water Research*, *43*(9), 2399–2408. doi: 10.1016/j.watres.2009.03.009

Yu, Q., Zhang, R., Deng, S., Huang, J., & Yu, G. (2009). Sorption of perfluorooctane sulfonate and perfluorooctanoate on activated carbons and resin: Ki-

netic and isotherm study. *Water Research*, *43*(4), 1150–1158. doi: 10.1016/j.watres.2008.12.001

Zhang, W., & Elliott, D. W. (2006). Applications of iron nanoparticles for groundwater remediation. *Remediation Journal*, *16*(2), 7–21. doi: 10.1002/rem.20078

Zhu, P., Ling, X., Liu, W., Kong, L., & Yao, Y. (2016). Simple and fast determination of perfluorinated compounds in Taihu Lake by SPE-UHPLC-MS/MS. *Journal of Chromatography B*, *1031*, 61–67. doi: 10.1016/j.jchromb.2016.07.031

Appendix A

Additional Data From Chapter 2

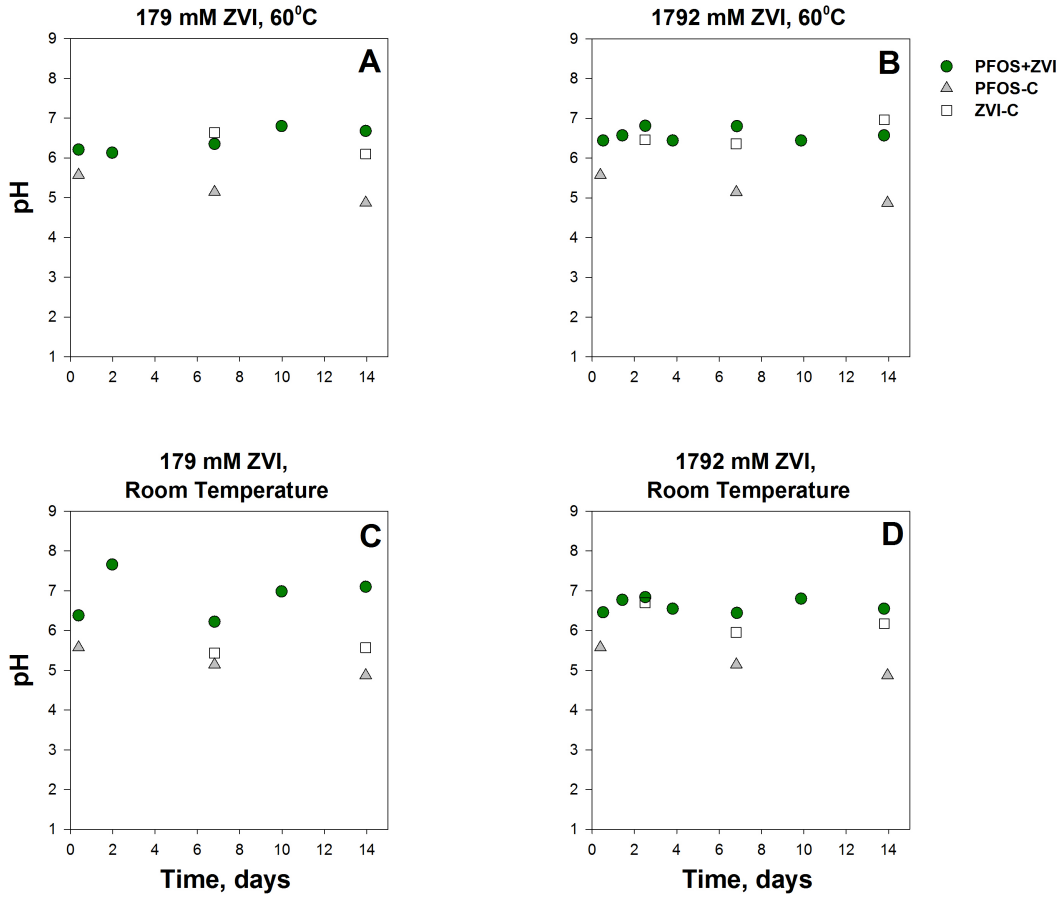

Figure A.1 Measured pH of aqueous treatment and control samples under pH_i 6.6 conditions. Figure A.1A) 179 mM ZVI, 60°C, B) 1792 mM ZVI, 60°C, C) 179 mM ZVI, room temperature, D) 1792 mM ZVI, room temperature. Initial pH is within 6.6 ± 0.4 while pH at later sampling times increases and remains within 7.0 ± 0.8 units for the remainder of the experiment.

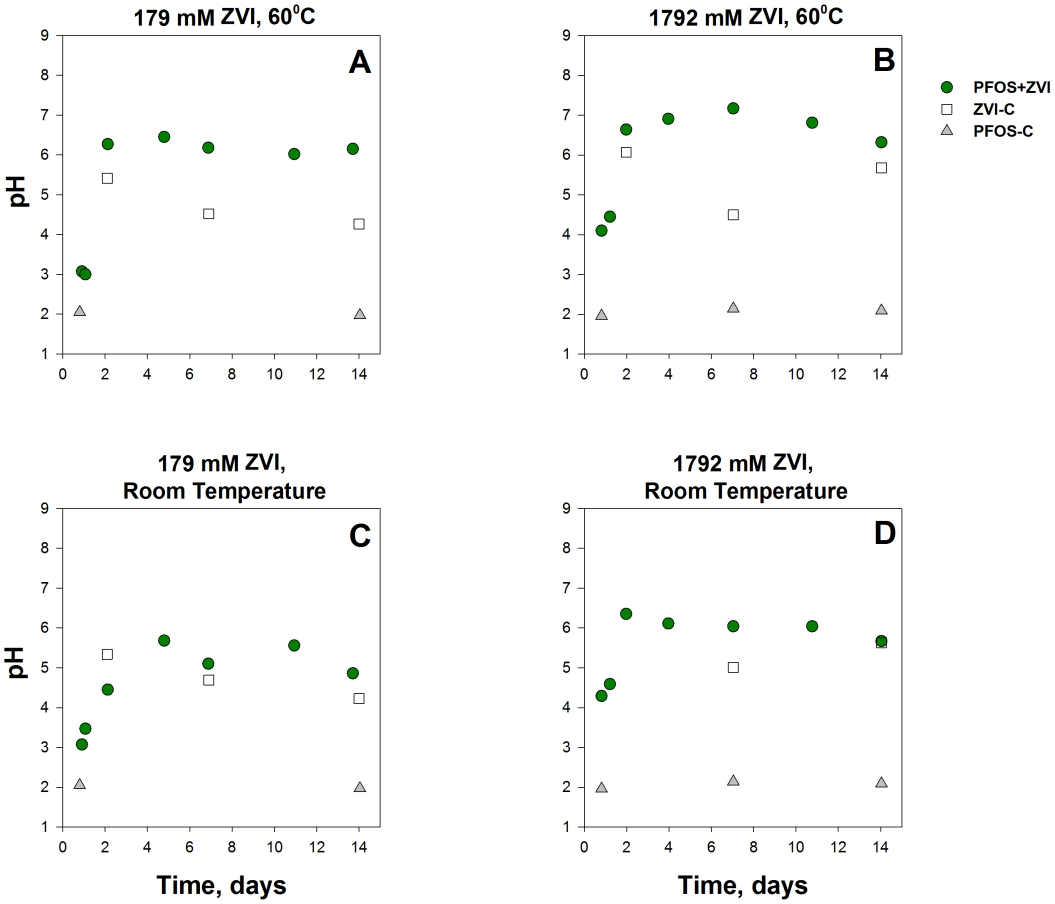

Figure A.2 Measured pH of aqueous treatment and control samples under pH_i 2.0 conditions. Figure A.2A) 179 mM ZVI, 60°C, B) 1792 mM ZVI, 60°C, C) 179 mM ZVI, room temperature, D) 1792 mM ZVI, room temperature. Initial pH is within 2 $\pm$ 0.3 while pH at later sampling times increases and remains within 6.1 $\pm$ 1.1 units after 4 days for the remainder of the experiment.

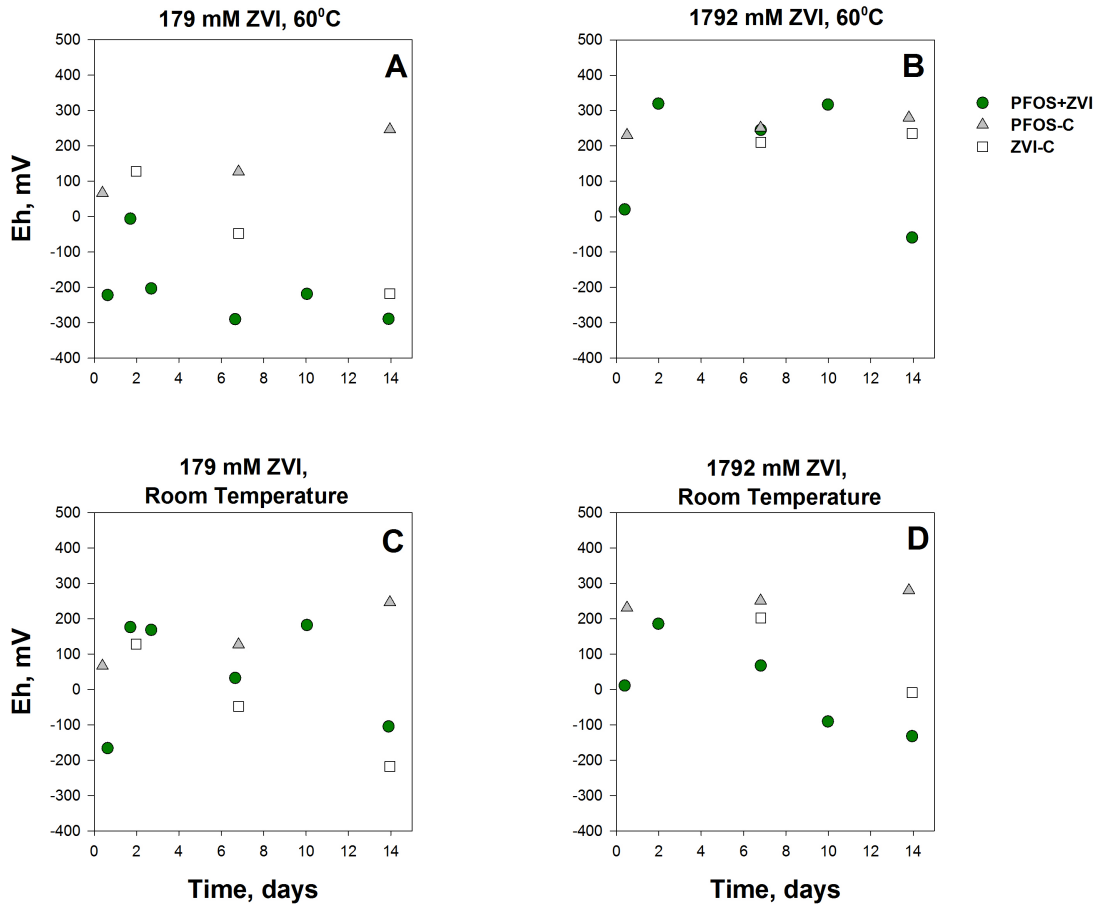

Figure A.3 Measured Eh of aqueous treatment and control samples under pH_i 6.6 conditions. Figure A.3A) 179 mM ZVI, 60°C, B) 1792 mM ZVI, 60°C, C) 179 mM ZVI, room temperature, D) 1792 mM ZVI, room temperature. All measurements were performed in the glovebox with the final value recorded when a point of inflection was achieved or 30 minutes had passed.

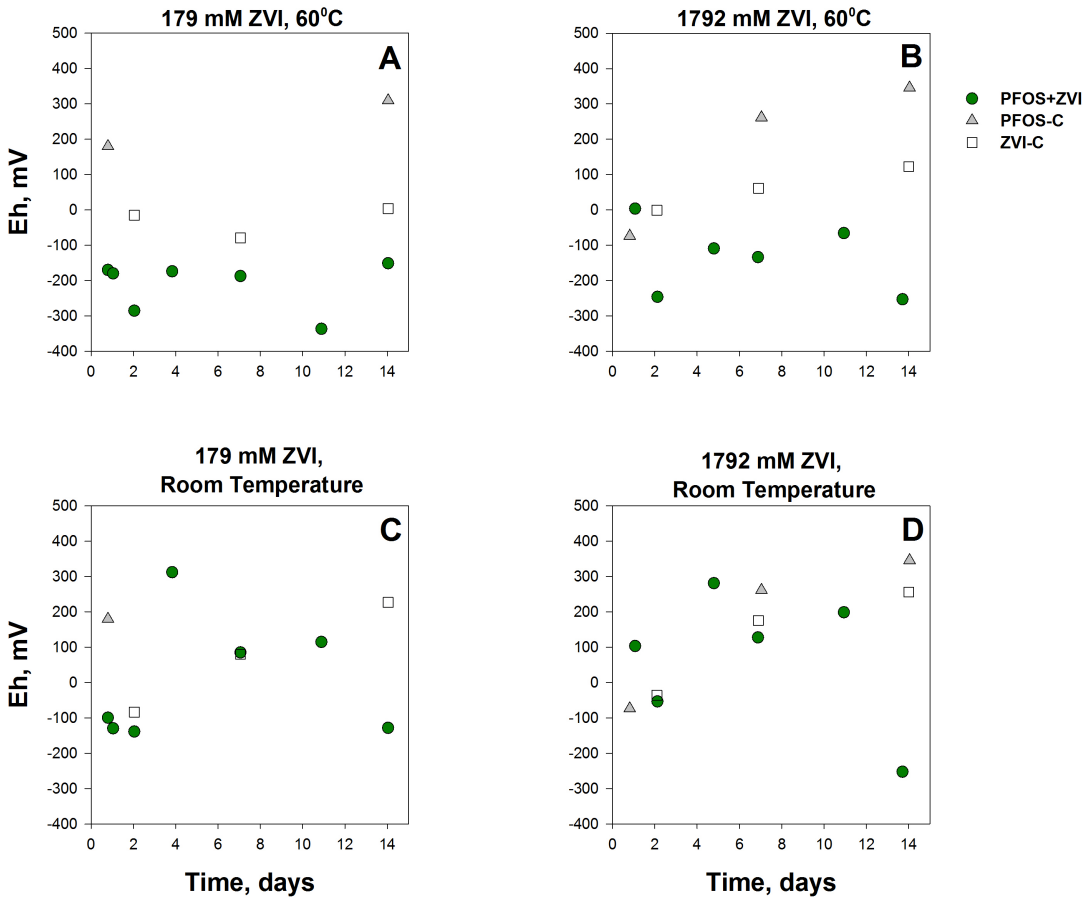

Figure A.4 Measured Eh under pH_i 2.0 conditions. Figure A.4A) 179 mM ZVI, 60°C, B) 1792 mM ZVI, 60°C, C) 179 mM ZVI, room temperature, D) 1792 mM ZVI, room temperature. All measurements were performed in the glovebox with the final value recorded when a point of inflection was achieved or 30 minutes had passed.

Table A.1 Calculated relative standard error of measured PFOS post HPLC-MS/MS analysis from multiple sources.

Source of Error	Minimum	Maximum	Mean	n
HPLC-MS/MS	0%	89%	8%	146
SPE + HPLC-MS/MS	0%	56%	11%	45
Duplicate Reactors + SPE + HPLC-MS/MS	2%	53%	16%	21
Triplicate Reactors + SPE + HPLC-MS/MS	4%	39%	25%	7

Table A.2 Quality control (QC) error of known PFOS concentration and its measured recovery post HPLC-MS/MS analysis.

QC (μg L^{-1})	**Minimum**	**Maximum**	**Mean**	**n**
0.5	33%	174%	101%	6
1	28%	185%	126%	12
2	59%	167%	107%	19
5	111%	159%	141%	23
10	78%	116%	98%	21
20	85%	147%	106%	26

Table A.3 Recovery of known PFOS concentration spiked in sample matrix and its measured recovery post HPLC-MS/MS analysis.

Spike (μg L^{-1})	**Minimum**	**Maximum**	**Mean**	**n**
0.5	68%	74%	71%	6
1	62%	73%	68%	7
2	82%	92%	87%	4
5	88%	95%	92%	3

Appendix B

Additional Data From Chapter 3

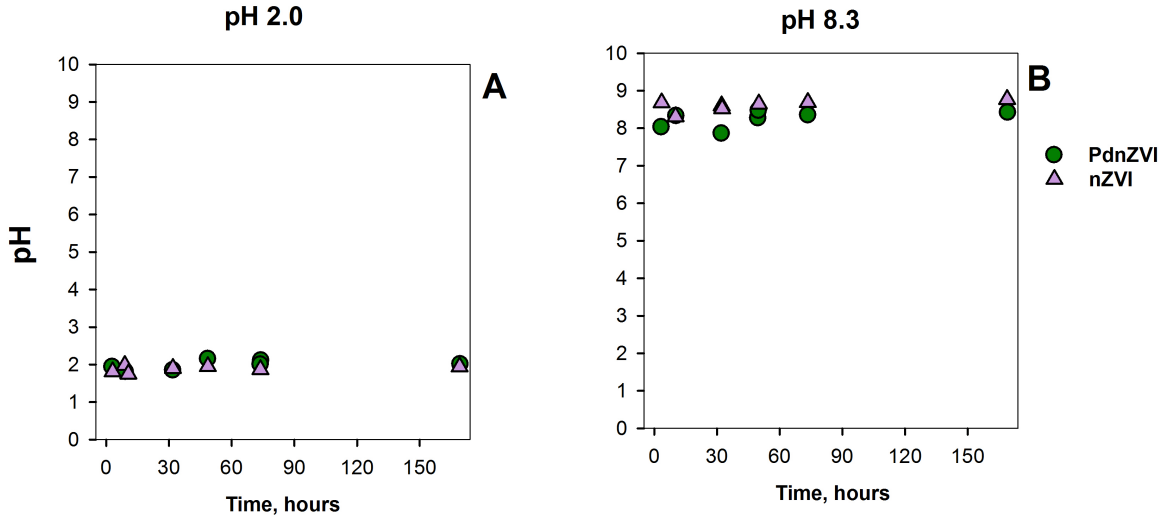

Figure B.1 Measurements of pH of the aqueous phase throughout the treatment period in the presence of PdnZVI and nZVI. Figure B.1A) pH 2.0, B) pH 8.3. All measurements were performed in the glovebox. Initial pH 2.0 remained within pH 2.0 $\pm$ 0.2 throughout the treatment period for both PdnZVI and nZVI. Uncontrolled pH remained within pH 8.3 $\pm$ 0.4 for both PdnZVI and nZVI.

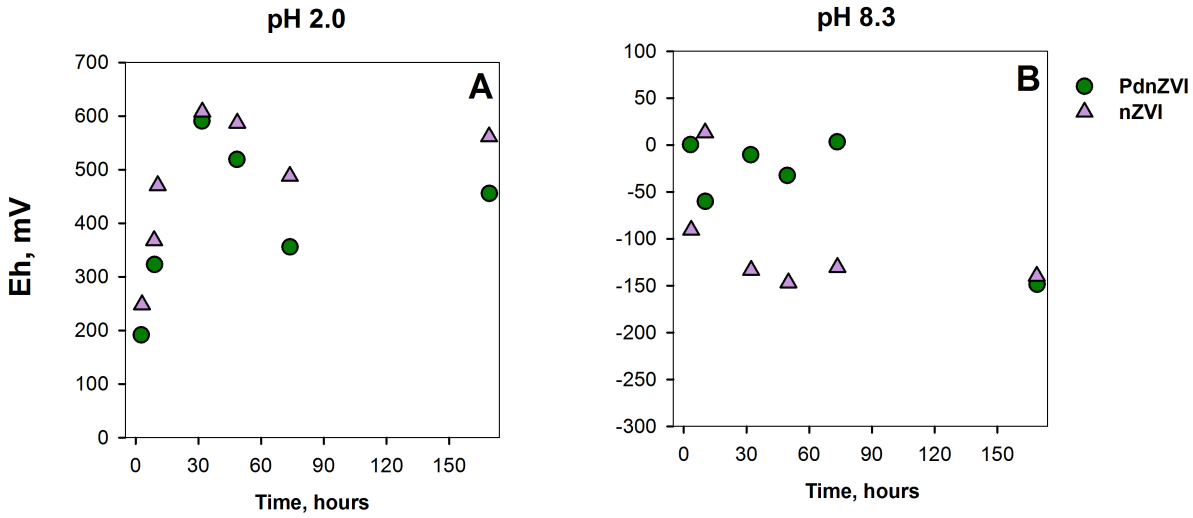

Figure B.2 Measurements of Eh of the aqueous phase throughout the treatment period in presence of PdnZVI and nZVI. Figure B.2A) pH 2.0, B) pH 8.3. All measurements were performed in the glovebox with the final value recorded when a point of inflection was achieved or 30 minutes had passed.

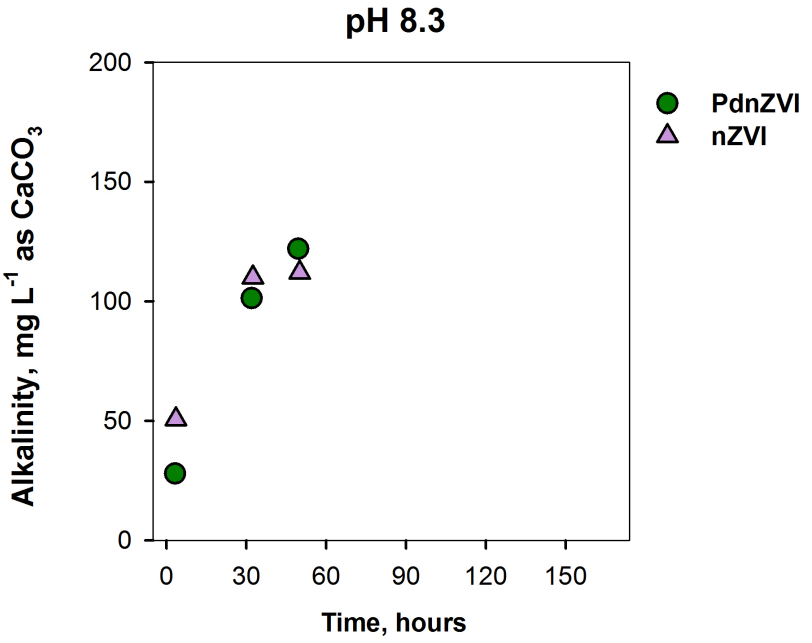

Figure B.3 Measurements of the alkalinity of the aqueous phase throughout the treatment period in the presence of PdnZVI and nZVI. All measurements were performed in the glovebox. Aqueous samples were titrated with 0.16 N H_2SO_4 to calculate digits, which was converted to alkalinity represented in mg L^{-1} as $CaCO_3$. No amount of alkalinity was observed for pH 2.0 at any sampling point.

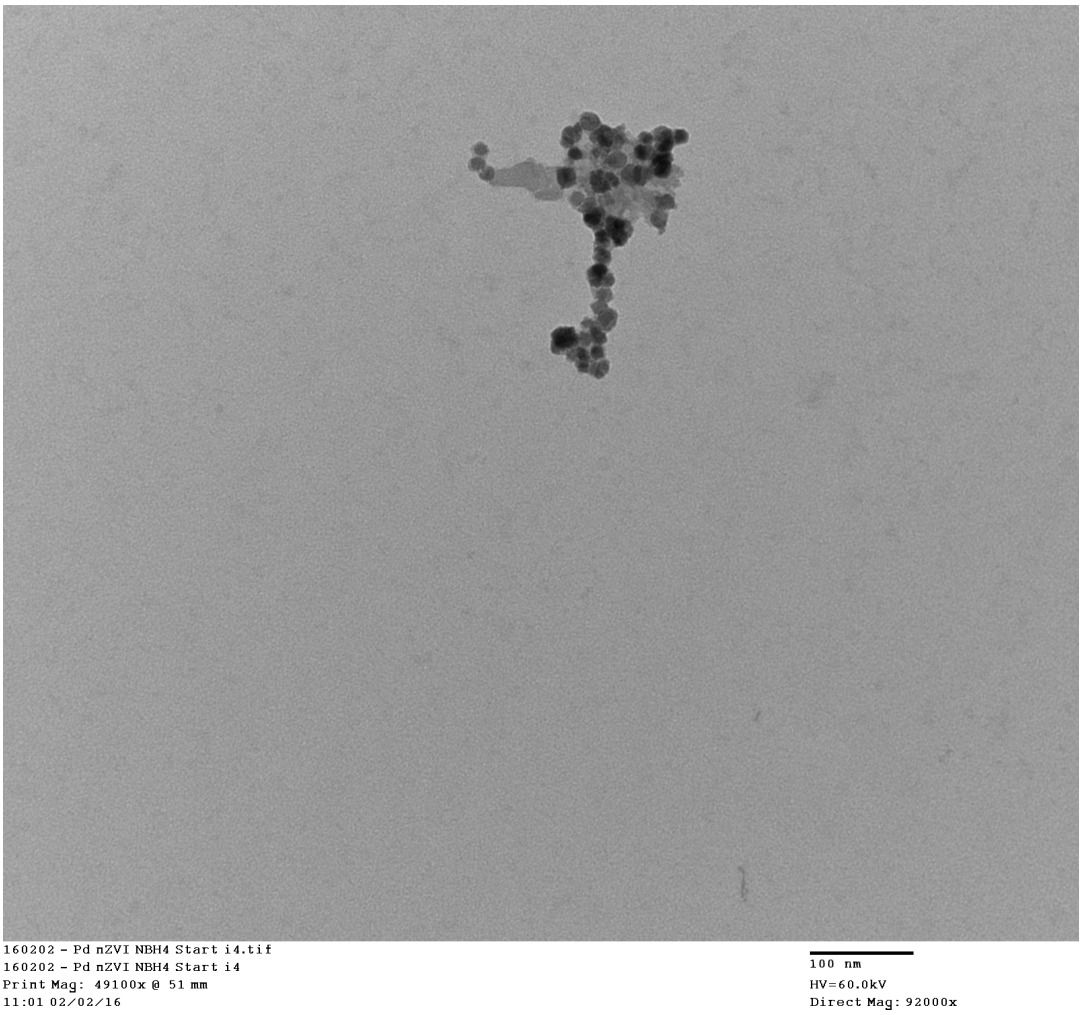

Figure B.4 Image of a sample of synthesized PdnZVI prior to use in batch experiments taken using transmission electron microscopy (TEM). High voltage was set at 60 kV. The direct magnification factor is 92,000.

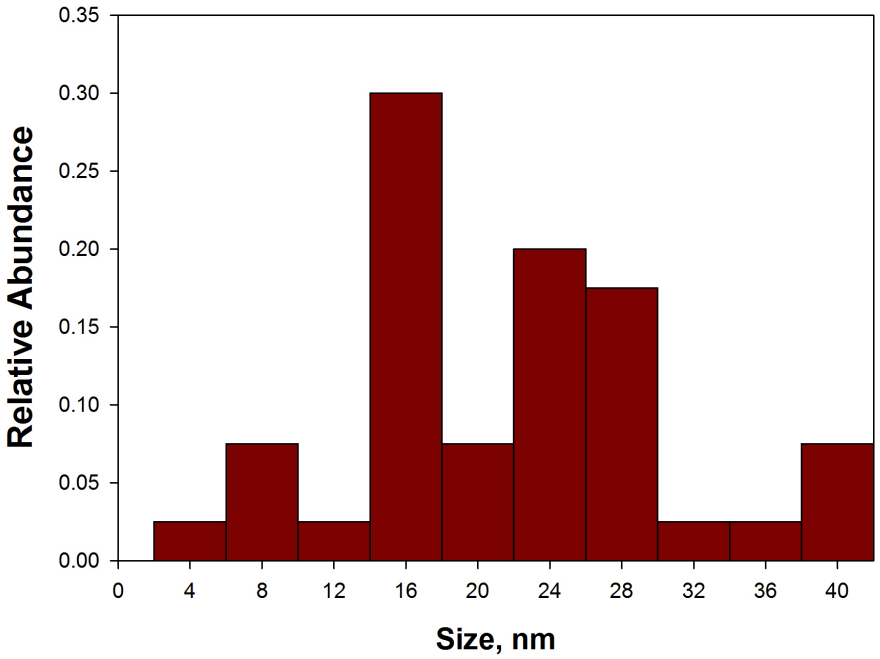

Figure B.5 The size distribution of synthesized PdnZVI. Size distribution was determined using ImageJ processing of Figure B.4. Nanoparticle sizes are classed within groups representing the midpoint across a range of 4 nm (e.g. 8 nm represents nanoparticles 8 ± 2 nm).